Synthesis, Microstructure and Properties of Metallic Materials with Nanoscale Growth Twins

X. Zhang*
Dept. of Mechanical Engineering, Texas A&M University,
College Station, Texas 77843-3123, zhangx@tamu.edu, 979-845-2143 (O)

A. Misra and R. G. Hoagland
Materials Science and Technology Division, Los Alamos National Laboratory,
Los Alamos, NM 87545

ABSTRACT

We have recently synthesized 330 stainless steel thin films and bulk Cu foils via magnetron sputtering with an average twin spacing of ~ 5 nm. Twin interfaces in both systems are of {111} type and normal to the growth direction. The hardness of sputtered materials is an order of magnitude higher than that of their bulk counterparts. Growth twins with such high twin density and preferred orientation are rarely seen in elemental metals. Sputtered Cu foils exhibited tensile strengths of 1.2 GPa, a factor of 3 higher than that reported earlier for nanocrystalline Cu, average uniform elongation of 1-2% and ductile dimple fracture surfaces. This work provides a new route for the synthesis of ultra-high strength, ductile metals via control of twin spacing and twin orientation in vapor-deposited materials.

1. INTRODUCTION

The mechanical properties of nanocrystalline metal have been studied extensively due to the high strengths achievable in these materials. For instance, the strength of single-phase metallic materials with equiaxed grains can be increased by an order of magnitude or higher when their grain sizes are reduced from tens of micrometers to 10 nanometers. However, at grain sizes below 10 nm, deformation mechanisms may involve grain boundary mediated plasticity (grain boundary sliding or rotation), and a reduction of strength with decreasing grain size has been predicted (Swygenhoven, 2002; Schiotz et al, 1998; Yip, 1998; Cheng et al, 2003; Schiøtz and Jacobsen, 2003; Van Vliet et al, 2003; Yip, 2004; Hasnaoui et al, 2003; Wei and Anand, 2004; Yamakov et al, 2002; Sansoz and Molinari, 2005). There is direct and indirect experimental evidence for the transition of deformation mechanisms (Schuh et al, 2002; Youngdah et al, 2001; Kumar et al, 2003; Sanders et al, 1997; Shan et al, 2004; Milligan et al, 1993; Ke et al, 1995) dependent upon grain sizes. The occurrence of high strength in nanocrystalline (grain size less than 100 nm) metallic materials is very often accompanied with low ductility, much lower than their bulk counterparts (Koch et al, 1999). The observed low ductility could be related to porosity due to incomplete compaction of nanocrystalline (nc) particulates (Koch et al, 1999). New synthesis routes are needed to produce single-phase metals that exhibit ultra-high strength and room temperature tensile ductility without a drop in strength with decreasing size in the nanometer regime.

Recently, Lu *et al*. reported high yield strength, 900 MPa, and room-temperature tensile ductility in electro-deposited Cu, with grain sizes varying from 100 to 1000 nm and an average grain size of 400 nm (Lu et al, 2004; Shen et al, 2005).

Most grains contained growth twins with the twin lamellae thickness varying from several nanometers to 150 nm, with a peak in twin size distribution at 15 nm (Lu et al, 2004; Shen et al, 2005). The high strength was presumed to result primarily from twins that had a finer length scale as compared to grains. High-density of twins have also been reported recently in electro- or vapor-deposited low-stacking fault energy alloys such as Ni-Co, Ni-Mn (Yang et al, 2004: Wu et al, 2005) and austenitic stainless steels (Zhang et al, 2004a; Zhang et al, 2005).

However, processing routes to produce nanoscale growth twins in materials in a controlled manner have not been developed. Deliberate tailoring, via control of processing parameters, of the nano-twinned structures is needed to fully exploit the potential of twin interfaces in producing high-strength materials with room temperature tensile-ductility. Specifically, this refers to the control of the thickness of the twin lamellae, spacing between adjacent twins and orientation of twin interfaces with respect to the growth direction. In this paper, we will overview our recent studies on the production of preferred-oriented, nano-twinned structures in single phase 330 stainless steel (330 SS) thin films and pure Cu foils via high-rate magnetron sputter deposition, hardness and strengthening mechanisms of nano-twinned metallic thin films, and the tensile properties of these nano-twinned Cu foils.

Report Documentation Page

Form Approved
OMB No. 0704-0188

1. REPORT DATE **01 NOV 2006**	2. REPORT TYPE **N/A**	3. DATES COVERED **-**
4. TITLE AND SUBTITLE **Synthesis, Microstructure and Properties of Metallic Materials with Nanoscale Growth Twins**		5a. CONTRACT NUMBER 5b. GRANT NUMBER 5c. PROGRAM ELEMENT NUMBER
6. AUTHOR(S)		5d. PROJECT NUMBER 5e. TASK NUMBER 5f. WORK UNIT NUMBER
7. PERFORMING ORGANIZATION NAME(S) AND ADDRESS(ES) **Dept. of Mechanical Engineering, Texas A&M University, College Station, Texas 77843-3123**		8. PERFORMING ORGANIZATION REPORT NUMBER
9. SPONSORING/MONITORING AGENCY NAME(S) AND ADDRESS(ES)		10. SPONSOR/MONITOR’S ACRONYM(S) 11. SPONSOR/MONITOR’S REPORT NUMBER(S)
12. DISTRIBUTION/AVAILABILITY STATEMENT **Approved for public release, distribution unlimited**		
13. SUPPLEMENTARY NOTES **See also ADM002075., The original document contains color images.**		
14. ABSTRACT		
15. SUBJECT TERMS		

16. SECURITY CLASSIFICATION OF:			17. LIMITATION OF ABSTRACT	18. NUMBER OF PAGES	19a. NAME OF RESPONSIBLE PERSON
a. REPORT	b. ABSTRACT	c. THIS PAGE			
unclassified	**unclassified**	**unclassified**	**UU**	**37**	

Standard Form 298 (Rev. 8-98)
Prescribed by ANSI Std Z39-18

2. EXPERIMENTAL

A Cu (99.999%) and a face-centered cubic (fcc) 330 SS material (43 wt% Fe, 18wt% Cr, 36wt% Ni, 2wt% Mn, 0.08wt% C) target were sputtered respectively using magnetron sputtering deposition technique. 330 SS films with a few micron thickness, and Cu coatings, 20 µm thick, were deposited on oxidized silicon substrates. The chamber was evacuated to a base pressure of $\leq 5 \times 10^{-8}$ torr prior to deposition. No heating or cooling was applied to the substrate during deposition. The deposition rate was varied in the range of 0.5 - 2.0 nm/s by controlling the dc power to the magnetron gun. The hardness and indentation modulus of multilayers were measured, at room temperature, by means of an indentation load and depth sensing apparatus, a commercial Nano Indentor II, with a Berkovich indenter. High resolution transmission electron microscopy (HRTEM) was performed on a JEOL 3000F microscope operated at 300kV. The as-deposited Cu foils were peeled off from Si substrates and cut into dogbone-shaped specimens using electro-discharge machining for tensile tests. The gauge length of the tensile specimen was 4 mm with a width of 2 mm. Uniaxial tensile tests were performed on a Tytron 250 microforce testing system (MTS) at a strain rate of 6×10^{-3} s^{-1} at room temperature. A MTS LX300 laser extensometer was used to calibrate and measure the sample strain upon loading. The fracture surfaces of tensile specimens were examined with a JEOL 6400F scanning electron microscope.

3. RESULTS AND DISCUSSIONS

3.1 Microstructure and mechanical properties of sputter-deposited 330 SS thin films.

A low magnification bright field cross-section transmission electron microscopy (TEM), Fig. 1a, shows an average columnar grain size of around 30 nm with extremely high density twinning within the columnar grains. The average twin spacing is estimated to be around 4 nm. A cross-section high resolution transmission electron microscopy (HRTEM) image of this coating is shown in Fig.1b, with the corresponding diffraction pattern shown in the inset. A high density of growth twins on {111} planes with nanoscale twin spacing is observed with the twin interfaces parallel to the substrate surface. High density twinning in 330 SS with nanoscale spacing is also observed in 330 SS within Cu/330 SS multilayers. Details on microstructure of Cu/330 SS can be found elsewhere (Zhang et al, 2004b).

The hardness of these films, as measured by nanoindentation, is 6.5 ± 0.3 GPa, very high compared with the yield strength of ~200 MPa for bulk SS330. The hardness results are reproducible. Hardness tests on different types of substrates, GaAs, Sapphire, glass and Si (100), yield the same results and the same nanoscale twinned structures in SS330 films.

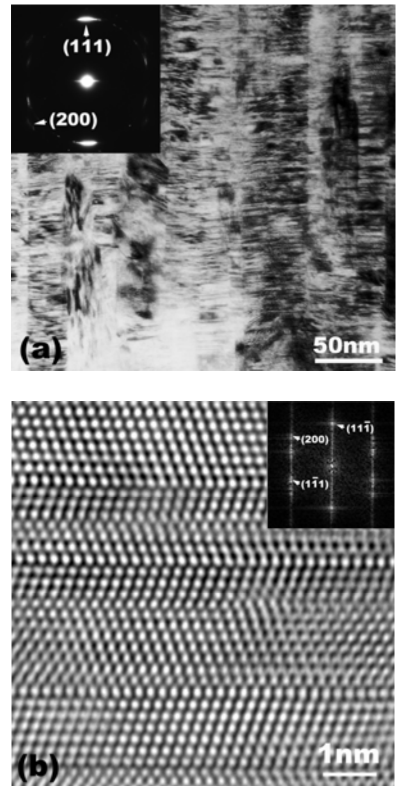

Fig. 1 (a) Bright field TEM of 330 SS films with an average columnar grain size of around 30 nm, showing high density twinning within the columnar grains. (b) HRTEM image showing nanoscale growth twins on {111} in sputtered 330 stainless steel films. The inset showing fast Fourier transform from the corresponding image.

Early work (Babyak and Rhines, 1960) showed that annealing twin boundaries are equivalent to grain boundaries in providing Hall-Petch type strengthening in α-brass where grain (or twin) boundary spacing is in the few to a few tens of micrometers range. Methods such as high-rate (> 10 nm /s) physical vapor deposition of copper (Merz and S. D. Dahlgren, 1975) and nickel (Dahlgren et al, 1977) and shock loading of stainless steels (Murr et al, 1978) have produced twin structures with spacing in the range of few tens to hundreds of nm.

Hall-Petch behavior, where dislocation pile-ups form at grain (or, in this case, twin) boundaries leading to hardness proportional to $L^{-1/2}$, (L is the twin spacing), is observed in these materials, as shown in Fig. 2 for stainless steels. The data points on 316 SS twinning strengthening come from (Murr et al, 1978), while on 316 SS grain boundary strengthening come from (Kashyap and Tangri, 1995; Kurzydlowski et al, 1996). For comparison, the datum point from the present work on nanoscale twinned SS330 is also shown here. The current comparisons are reasonable based on the fact that mechanical properties (hardness, yield strength, tensile strength) of bulk austenitic stainless steel (304, 310, 316 and 330) are quite similar and the lack of literature data on grain boundary strengthening in 330 SS, especially for grain sizes in the tens to hundreds of nm. While the decrease in twin spacing from ~100 nm to 4 nm has resulted in significant increase in hardness, the Hall-Petch model extrapolation fails to explain the high hardness of the 4 nm twin spacing sample. The transmission of single glide dislocations across the twin boundaries, as opposed to the formation of dislocation pile-ups, is the likely mechanism for yielding in such fine-scale structures (Rao and Hazzledine, 2000; Misra et al, 2002, Hoagland et al, 2002).

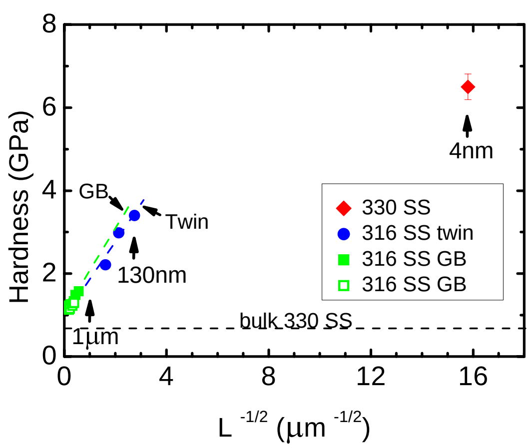

Fig. 2. Hardness vs. $L^{-1/2}$ for twinning-strengthened 316 SS (marked by solid circle), grain boundary strengthened 316SS (marked by solid square) (marked by open square) and current study for 330 SS (marked by solid diamond). L stands for the twin spacing for data from ref. (Murr et al, 1978) and sputtered 330 SS films, while it stands for the average grain size for data from ref. (Kashyap and Tangri, 1995; Kurzydlowski et al, 1996). Horizontal dashed line indicates the typical hardness for bulk 330 SS.

To explore the strengthening mechanisms in nanoscale twinned 330 SS films, we have simulated the transmission of a dislocation through a twin interface at the atomic scale in an fcc metal by means of molecular dynamics (MD) using an EAM interatomic potential for Ni. In Fig. 3a, the upper and lower lattices are in a $\sum 3$ twin orientation with respect to each other and the twin interface is a symmetric (111) plane. The models were periodic in the direction parallel to the dislocation line, which was straight, and had fixed boundary conditions in the other two directions.

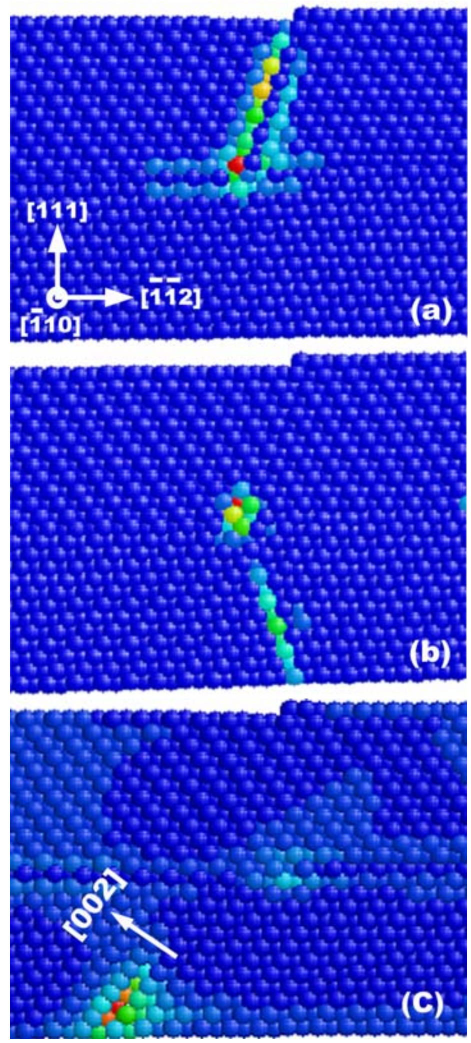

Fig. 3. An atomistic model containing a symmetric 3 {111} twin, the interface of which is horizontal. Atoms are colored by their excess energy relative to perfect unstrained crystal with blue lowest and red, highest. (a). A perfect glide dislocation with b = 1/2 [101] is on the upper {111} plane in the model near the interface. (b) The model is subjected to pure shear stress such that the resolved shear stress on the dislocation is 1.77GPa. The dislocation is moving across and then away from the twin interface onto the lower {111} planes. A Shockley partial with b = 1/6 $[\bar{1}\bar{1}2]$ remains at the interface. (c) In response to a biaxial stress (tension or compression in a plane parallel to the interface) that exerts a resolved shear stress of 3 GPa, a dislocation moves away from the interface into the lower grain on a {200} plane, leaving a Shockley at the interface. Note that the Shockley has also moved slightly along the interface plane toward the right side of the model.

Although fixed, the boundaries contained the displacement field of a dislocation near the interface.

Thus, image forces on the dislocation due to incompatibility between the dislocation position defining the boundary atom displacements and the actual position of the dislocation core were very small or negligible when interface crossing occurs. The models were two periods thick in the periodic direction and were otherwise fully 3D. In Fig. 3, atoms are colored by their excess energy ranging from blue as lowest to red as highest excess energy relative to the perfect unstrained crystal. In all figures the view is parallel to the dislocation line (out of the paper). A perfect dislocation with b = 1/2 [101], resides on the {111} plane in the upper crystal.

Two types of loading conditions or stress states were applied to understand the influence of twin boundaries on the transmission of a single dislocation. In the first case, as shown in Fig. 3b, the crystal is subjected to pure shear stress. When the resolved shear stress reach ~ 1.7 GPa, the dislocation will move across the twin interface into the lower crystal on the corresponding {111} glide planes. The Burgers vector changes as the dislocation moves onto the complementary glide plane in the lower layer. Consequently, a Shockley partial with b = 1/6 $[\bar{1}\bar{1}2]$ remains at the interface after the perfect dislocation crosses the twin interface.

In the second case, the model is subjected to a biaxial stress (tension or compression). Applying a biaxial stress in a plane parallel to the twin interface, (the normal stress in the direction perpendicular to the interface is zero), produces a resolved shear stress on this dislocation that exerts a force toward the twin interface. If this dislocation is placed on the corresponding {111} slip plane in the lower crystal, the same stress state exerts a force that is also toward the interface. For this reason, it is not possible for the dislocation in Figure 4a to cross the interface from the upper crystal and move onto the {111}glide planes in the lower crystal as it did in the first case. Instead, at a very large resolved shear stress of about 3 GPa, the dislocation enters the lower crystal on a {200} plane. The resolved shear stress to accomplish this dislocation crossing event is almost double the 1.7 GPa required to transmit slip in the first case. It is known that the critical resolved shear stress for slip to occur on a non-closely packed plane in fcc crystals, such as {200} is typically higher than that of a closely packed {111} plane. These studies reveal that the resistance of twin interface to transmission of dislocations depends sensitively on the stress state.

The current simulation was performed at 0K. Although the resolved shear stress should be decreased as a result of thermal activation at room temperature, the simulation results capture the essence that twin boundaries can be very strong obstacles to transmission of single dislocations. Dislocation pile-ups would form at higher twin spacing, and the stress concentration from the pile-up would allow slip transmission across twin boundary at a lower applied stress, thereby reducing the strength of the material. Therefore, nanoscale spacing of twins is critical in achieving the high strength in 330 SS thin films.

3.2. Microstructure and mechanical properties of sputter-deposited Cu foils.

Transmission electron microscopy (TEM) was used to characterize the microstructure of the as-deposited Cu foils with 20 micrometers total thickness. As shown in the cross-section TEM image in Fig. 4a, Cu sputter-deposited at a rate of 1.8 nm/s, exhibits a {111} fiber texture along the growth direction and an average columnar grain size of 43 nm.

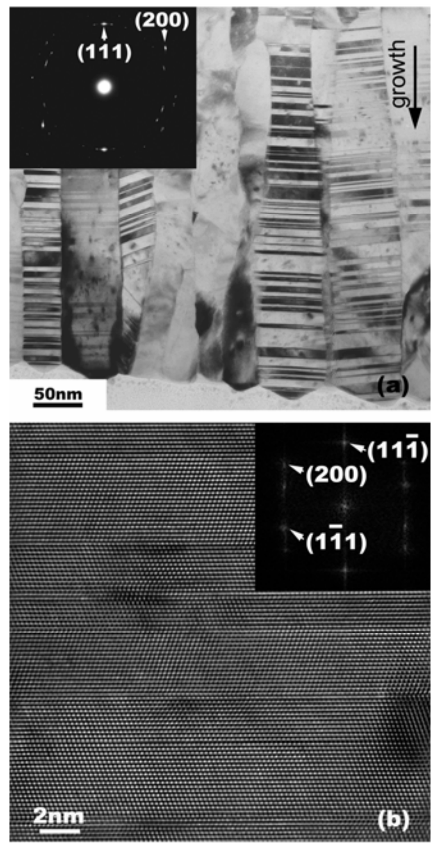

Fig. 4. (a) Cross-sectional TEM micrograph of Cu sputter-deposited at a deposition rate of 1.8 nm/s. The Cu film has an average columnar grain size of approximately 43 nm filled with a high density of planar defects parallel to the substrate surface. (b) HRTEM micrograph of the same specimen showing that the planar defects are growth twins with {111} interfaces. The inserted fast Fourier transform of the image shows spot-splitting across the {111} twin interfaces. Some stacking faults are also seen in HRTEM micrographs.

The average columnar grain size of Cu varied from 43 nm to 80 nm with deposition rates from 1.8 nm/s to 3 nm/s, respectively. Fig. 4 also shows an extremely high density of planar defects within the columnar grains, observed at all deposition rates from to 0.5 to 3nm/s. High-resolution TEM (HRTEM) imaging (Fig. 4b) of these planar defects reveals these to be several {111} twin interfaces separated by a few nanometers. {111} diffraction spot-splitting seen in the fast Fourier Transform of the HRTEM image in Fig. 4b is consistent with {111} twin interfaces. Most growth-twin interfaces are parallel to the film surface. Some planar faults were identified to be stacking faults.

Statistical measurement of the twin thickness and spacing from several TEM images indicate that the average twin thickness is 4 nm, whereas the average spacing between adjacent twins is also on the same order, approximately 5 nm (Fig.5). The narrow size distributions for both twin thickness and spacing are evident from Fig. 5, with very few twins exceeding 10 nm dimensions.

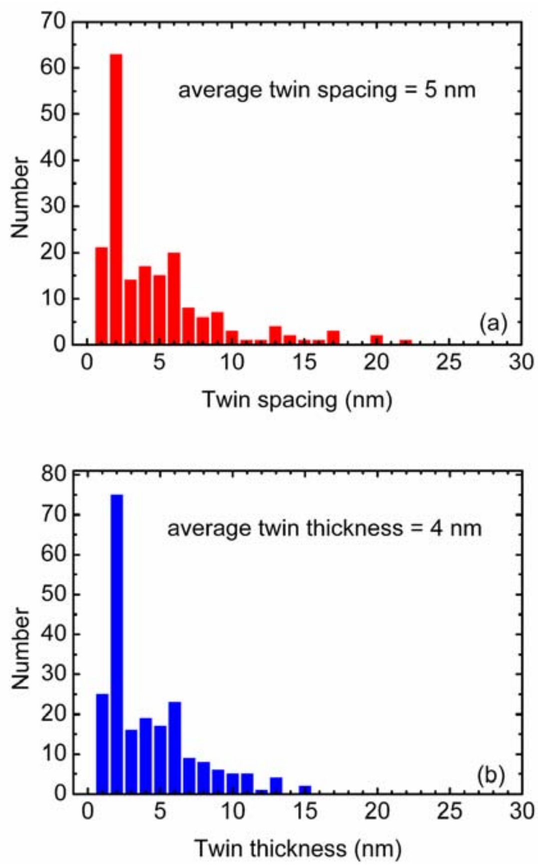

Fig. 5. Statistical measurements from TEM images showing that (a) the average twin spacing in Cu sputter-deposited at a deposition rate of 1.8 nm/s is approximately 5nm, and (b) the average twin thickness is 4 nm.

Five uniaxial tensile tests were performed on free-standing 20 micrometers thick Cu foils. The results were very reproducible, and a typical true stress – true total strain curve is shown in Fig. 6. A clear yield point is not observed in the stress-strain curves, so the yield strength was obtained as 0.2% offset to be 1.05 GPa, with an average value of 1.1 GPa estimated from 5 specimens. The elastic modulus is estimated to be approximately 110 GPa. Tensile strength, averaged over 5 tests, was 1.2 GPa and average true strain to failure was 2%.

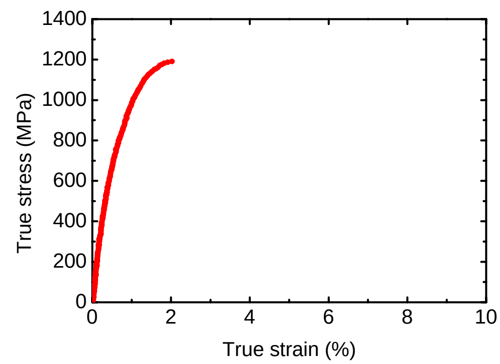

Fig. 6. True stress vs. true total strain curve for tensile tested Cu foils (20 μm) sputter-deposited at a deposition rate of 1.8 nm/s. The specimens have an average yield strength of 1.1 GPa and an elastic modulus of approximately 110 GPa.

The hardness, as measured by nanoindentation, was 3.5 GPa and, following the Tabor relation [26], approximately a factor of 3 higher than the tensile strength. The fracture surface of the Cu specimen shows typical ductile dimples as examined by SEM, shown in Fig. 7. Most dimples have diameters of one micron or less, much larger than the columnar grain diameters of 40-80 nm.

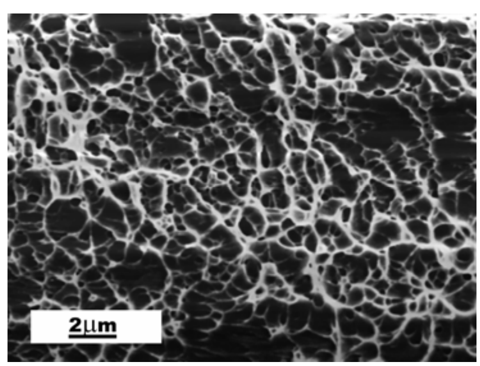

Fig. 7. SEM micrograph of the fracture surface of tensile tested nano-twinned Cu showing dimples indicative of a ductile fracture mode.

Room temperature tensile strengths reported for nc Cu are typically 400-500 MPa, with reported grain sizes ranging from 20 nm to greater than 100 nm. For inert gas condensed and compacted Cu, Sanders *et al*. (Sanders et al 1997) reported the highest tensile strength of 480 MPa for an average grain size of 22 nm by testing different samples with average grain sizes ranging from 16 nm to 110 nm, and Champion *et al*. (Champion et al, 2003) reported tensile strength of 400 for average grain size of 80 nm. For nc Cu produced by severe plastic deformation, Wang *et al*. (Wang et al 2002) and Valiev *et al*. (Valiev et al 2002) reported tensile strength of 450 - 500 MPa for grain sizes < 200 nm. The tensile strength of 1.2 GPa observed in the present investigation for an average columnar grain size of 43 nm is almost a factor of three higher than the highest tensile strength reported for nc-Cu, with the exception of the electro-deposited Cu with high twin density (Shen et al 2005). The yield strength of our sputtered Cu, 1.1 GPa, is the highest among all elemental Cu reported to date. Since the average twin thickness and spacing of approximately 5 nm are an order of magnitude smaller than the grain size, we hypothesize that the strength of the sputter-deposited Cu is controlled predominantly by the nanoscale twins, with relatively minor contributions from grain size and grain orientation (texture). This is consistent with our molecular dynamics simulations, published elsewhere (Zhang et al 2004a; Zhang et al, 2005), that have shown that twin boundaries can act as effective barriers to slip transmission. A very high resolved shear stress of 1.7 GPa was needed in the 0 K simulation to transmit a single dislocation across twin interfaces in Ni constructed with embedded-atom-method potential. Besides the thickness of individual twins and spacing between twins, another important feature is the alignment of twin boundaries parallel to the tensile axis. Thus, macroscopic plastic deformation of the sample requires slip transmission across the 5 nm spaced twin boundaries for all active slip systems. The nano-twinned Cu foils, with yield strength in excess of 1 GPa, also exhibit 1- 2% uniform elongation at room temperature. Typically, for nc-metals with grain sizes below ≈ 20 nm, insignificant tensile ductility is observed. Earlier reports of room-temperature tensile ductility in nc-Cu have been on materials with grain size of 200 nm or larger (Valiev et al 2002), or bimodal grain size distribution with coarser grains on the order of micrometers (Wang et al 2002) or very slow strain rate testing (10^{-6} /s) of samples with 80 nm average grain size (Champion et al, 2003). Our current results on sputter-deposited Cu are consistent with earlier work by our co-authors (Shen et al 2005) where room temperature tensile ductility was observed in electro-deposited Cu with a few tens of nanometers thick twins. As shown by MD simulations, each slip transmission event across a twin interface leaves behind a large residual Burgers vector at the interface that repels the next slip event on the same slip plane leading to work hardening. Under uniaxial tensile loading, geometrical instability (necking) is predicted when flow stress exceeds the work hardening rate, so in very high strength materials, large uniform elongations in tension are not expected. Nevertheless, the ductile failure mode of nano-twinned Cu is evident from Fig. 7.

The density of growth twins in sputter-deposited Cu may be interpreted in terms of a thermodynamic model developed for the formation of growth twins in sputter-deposited austenitic stainless steel thin films (Zhang et al, 2004b). The model predicts that the during vapor deposition twinned nuclei will form at rates comparable to defect-free nuclei if the free energy change from vapor to solid are comparable for the perfect and twinned nuclei. This happens when (i) the deposited material has low stacking fault and twin boundary energies, and (ii) the deposition rate is high. For Cu with a relatively low stacking fault energy of approximately 40 mJ/m^2, growth faults and twins are predicted to form at deposition rates of a nanometer/second or higher at room temperature. At elevated temperatures, higher surface diffusion leads to a higher probability of achieving the correct crystallographic orientation or packing sequence during deposition, and thus, a suppression of growth twin formation. Manipulation of the process parameters (deposition rate, substrate temperature) and material properties (stacking fault energy) provide a way to control twin densities during physical vapor deposition. The preferred orientation of the twins is a consequence of columnar grain morphology with {111} fiber texture produced during low homologous temperature physical vapor deposition.

Current studies of nanoscale growth twins in 330 SS and Cu films have yield certain similarities. (i) Both systems have similar microstructures: {111} type growth twins oriented predominantly parallel to substrate surface within columnar grains, and the average twin spacing in both systems are less than 10 nm (ii) The hardnesses (strength) of films are extraordinarily high compared to that of their bulk counterparts. (iii) Both systems have relatively low stacking fault energy. Furthermore it is noticed that the stacking fault energy of many metallic materials can be tailored via alloying. The strengthening mechanism discussed in the paper could therefore have more general indications for many other systems.

Future studies will explore mechanical (rolling) and thermal stability of these nanotwinned metal films, the formation mechanisms of nanoscale growth twins and electrical properties of nano-twinned metallic materials.

4. SUMMARY

We present a new perspective in strengthening metallic materials using nanoscale growth twins. Metallic films prepared by sputtering deposition techniques possess high density growth twins with preferred orientations, parallel to substrate surface. Twin interfaces act as strong barriers to the transmission of dislocations. Furthermore high strength metallic materials with nanoscale growth twins have certain ductility.

ACKNOWLEDGEMENTS

AM and RGH acknowledge financial support by the US DOE, Office of Science, Office of Basic Energy Sciences and Laboratory Directed R&D at LANL. Discussions with J. P. Hirth, J. D. Embury, T. E. Mitchell and M. Nastasi are gratefully acknowledged.

REFERENCES

W. J. Babyak and F. N. Rhines, Trans. Met. Soc. AIME, 1960: The Relationship Between the Boundary Area and Hardness of Recrystallized Cartridge Brass, T*RANSAC-TIONS OF THE AMERICAN INSTITUTE OF MINING AND METALLURGICAL ENGINEERS*, **218,** 21-23.

Y. Champion, C. Langlois, S. Guerin-Mailly, P. Langlois, J.L. Bonnentien, M.J. Hytch, 2003: Near-perfect Elastoplasticity in Pure Nanocrystalline Copper, *SCIENCE,* **300,** 310-311.

S. Cheng, J. A. Spencer, and W. W. Milligan, 2003: Strength and Tension/Compression Asymmetry in Nanostructured and Ultrafine-grain Metals, *ACTA MATERIALIA,* **51**, 4505-4518.

S. D. Dahlgren, W. L. Nicholson, M. D. Merz, W. Bollmann, J. F. Devlin and R. Wang, 1977: Microstructural Analysis and Tensile Properties of Thick Copper and Nickel Sputer Deposits, *THIN SOLID FILMS,* **40**, 345-353.

A. Hasnaoui, H. Van Swygenhoven, P. M. Derlet, 2003: Dimples on Nanocrystalline Fracture Surfaces as Evidence for Shear Plane Formation, *SCIENCE* **300**, 1550-1552.

B. P. Kashyap and K. Tangri, 1995: On the Hall-Petch Relationship and Substructural Evolution in Type 316L Stainless-Steel, *ACTA METALLURGICA ET MATERIALIA,* **43,** 3971-3981.

M. Ke, S. A. Hackney, W. W. Milligan, and E. C. Aifantis, 1995: Observation and Measurement of Grain Rotation and Plastic Strain in Nanostructured Metal Thin-Films, *NANOSTRUCTURED MATERIALS,* **5,** 689-697.

R.G. Hoagland, T.E. Mitchell, J.P. Hirth and H. Kung, 2002: On the Strengthening Effects of Interfaces in Multilayer fcc Metallic Composites, *PHILOSOPHICAL MAGAZINE A,* **82**, 643-664.

C. C. Koch, D. G. Morris, K. Lu, and A. Inoue, 1999: Ductility of Nanostructured Materials, *MRS BULLETIN,* **24**, 54-58.

K.S. Kumar, S. Suresh, M.F. Chisholm, J.A. Horton, P. Wang, 2003: Deformation of Electrodeposited Nanocrystalline Nickel, *ACTA MATERIALIA*, **51**, 387-405.

K. J. Kurzydlowski, B. Ralph, J. J. Bucki and A. Garbacz, 1996: The Grain Boundary Character Distribution Effect on the Flow Stress of polycrystals: The influence of Crystal lattice Texture, *MATERIALS SCIENCE AND ENGINEERING A*, **205**, 127-132.

L. Lu, Y. Shen, X. Chen, L. Qian, K. Lu, 2004: Ultrahigh Strength and High Electrical Conductivity in Copper, *SCIENCE,* **304**, 422-426.

M. D. Merz and S. D. Dahlgren, 1975: Tensile-Strength and Work-Hardening of Ultrafine-Grained High-Purity Copper, *JOURNAL OF APPLIED PHYSICS,* **46**, 3235-3237.

W. W. Milligan, S. A. Hackney, M. Ke, and E. C. Aifantis, 1993: In Situ Studies of Deformation and Fracture in Nanophase Materials, *NANO-STRUCTURED MATERIALS*, **2,** 267-276.

A. Misra, J. P. Hirth and H. Kung, 2002: Single-Dislocation-Based Strengthening Mechanisms in Nanoscale Metallic Multilayers, *PHILOSOPHICAL MAGAZINE A* **82**, 2935-2951.

L. E. Murr, E. Moin and F. Greulich, 1978: Contribution of Deformation Twins to Yield Stress – Hall-Pecth Law for Inter-Twin Spacing, *SCRIPTA METALLURGICA*, **12**, 1031-1035.

S. I. Rao and P. M. Hazzledine, 2000: Atomistic Simulations of Dislocation-Interface Interactions in the Cu-Ni Multilayer System, *PHILOSOPHICAL MAGAZINE A*, **80,** 2011-2040.

P.G. Sanders**,** J.A. Eastman, and J. R. Weertman, 1997: Elastic and Tensile Behavior of Nanocrystalline Copper and Palladium, *ACTA MATERIALIA*, **45,** 4019-4025.

F. Sansoz and J. F. Molinari, 2005: Mechanical Behavior of Σ Tilt Grain Boundaries in Nanoscale Cu and Al: A Quasicontinuum Study, *ACTA MATER*, **53**, 1931-1944.

J. Schiotz, and K. W. Jacobsen, 2003: A Maximum in the Strength of Nanocrystalline Copper, *SCIENCE,* **301,** 1357-1359.

J. Schiotz, F.D. Di Tolla and K. W. Jacobsen, 1998: Softening of Nanocrystalline Metals at Very Small Grain Sizes, *NATURE,* **391,** 561-563.

C. A. Schuh, T. G. Nieh and T. Yamasaki, 2002: Hall-Petch Breakdown Manifested in Abrasive Wear Resistance of Nanocrystalline Nickel, *SCRIPTA MATERIALIA,* **46,** 735-740.

Z. Shan, E.A. Stach, J.M.K. Wiezorek, J.A. Knapp, D.M. Follstaedt and S.X. Mao, 2004: Grain Boundary-Mediated Plasticity in Nanocrystalline Nickel, *SCIENCE,* **305,** 654-657.

Y.F. Shen, L. Lu, Q.H. Lu, Z.H. Jin, K. Lu, 2005: Tensile Properties of Copper with Nano-scale Twins, *SCRIPTA MATERIALIA*, **52,** 989-994.

D. Tabor, 1951: The Hardness of Metals, Oxford University Press, New York.

H. van Swygenhoven, 2002: Grain Boundaries and Dislocations, *Science*, **296,** 66-67.

R.Z. Valiev, I.V. Alexandrov, Y.T. Zhu and T.C. Lowe, 2002: Paradox of Strength and Ductility in Metals Processed by Severe Plastic Deformation, *JOURNAL OF MATERIALS RESEARCH*, **17**,5-8.

K. J. Van Vliet, S. Tsikata, and S. Suresh, 2003: Model Experiments for Direct Visualization of Grain Boundary Deformation in Nanocrystalline Metals *APPLIED PHYSICS LETTERS*, **83,** 1441-1443.

Y.M. Wang, M.W. Chen, F.H. Zhou, E. Ma, 2002: High Tensile Ductility in a Nanostructured Metal, *NATURE*, **419**, 912-915.

Y. J. Wei, and L. Anand, 2004: Grain-boundary Sliding and Separation in Polycrystalline Metals: Application to Nanocrystalline fcc Metals, *JOURNAL OF THE MECHANICS AND PHYSICS OF SOLIDS*, **52,** 2587-2616.

B.Y.C. WU, P.J. FERREIRA, and C.A. SCHUH, 2005: Nanostructured Ni-Co Alloys with Tailorable Grain Size and Twin Density, *METALLURGICAL AND MATERIALS TRANSACTIONS A*, **36A,** 1927-1936.

V. Yamakov, D. Wolf, S. R. Phillpot, and H. Gleiter, 2002: Grain-Boundary Diffusion Creep in Nanocrystalline Palladium by Molecular-dynamics Simulation, *ACTA MATERIALIA*, **50,** 61-73.

N.Y.C. Yang, T.J. Headley, J.J. Kelly, and J.M. Hruby, 2004: Metallurgy of High Strength Ni-Mn Microsystems Fabricated by Electrodeposition, *SCRIPTA MATERIALIA*, **51,** 761-766.

S. Yip, 1998: Nanocrystals - The Strongest Size, *NATURE*, **391,** 532-533.

S. Yip, 2004: Nanocrystalline Metals - Mapping Plasticity, *NATURE MATERIALS*, **3**, 11-12.

C.J. Youngdahl, J.R. Weertman, R.C. Hugo, H. Kung, 2001: Deformation Behavior in Nanocrystalline Copper, *SCRIPTA MATERIALIA*, **44,** 1475-1478.

X. Zhang, A. Misra, H. Wang, M. Nastasi, J. D. Embury, T. E. Mitchell, R. G. Hoagland and J. P. Hirth, 2004a: Nanoscale Twinning Induced Strengthening in Austenitic Stainless Steel *Appl. Phys. Lett.*, **84**, 1096-1098.

X. Zhang, A. Misra, H. Wang, T. D. Shen, M. Nastasi, T. E. Mitchell, J. P. Hirth, R.G. Hoagland and J. D. Embury, 2004b: Enhanced Hardening in Cu/330 Stainless Steel Multilayers by Nanoscale Twinning, *ACTA MATERIALIA*, **52,** 995-1002.

X. Zhang, A. Misra, H. Wang, A. L. Lima, M. F. Hundley, and R. G. Hoagland, 2005: Effects of Deposition Parameters on Residual Stresses, Hardness and Electrical Resistivity of Nanoscale Twinned 330 Stainless Steel Thin Films, *J. Appl. Phys*., **97**, 094302.

High-strength Sputter-deposited Metallic Thin Films with Nanoscale Growth Twins

X. Zhang[1], O. Anderoglu[1], A. Misra[2], J. G. Swadener[2], and R. G. Hoagland[2]

[1] Dept. Mechanical Engineering, Texas A&M University
[2] Mater. Sci. Tech. Div., Los Alamos National Laboratory

Outline

- Background
- Influence of sputtering deposition rate on twin formation in 330 stainless steel (330 SS) films
- Nanoscale growth twins in sputter-deposited Cu films

Mechanical Properties of Thin Films – MEMS, microcantilever beams, tribology

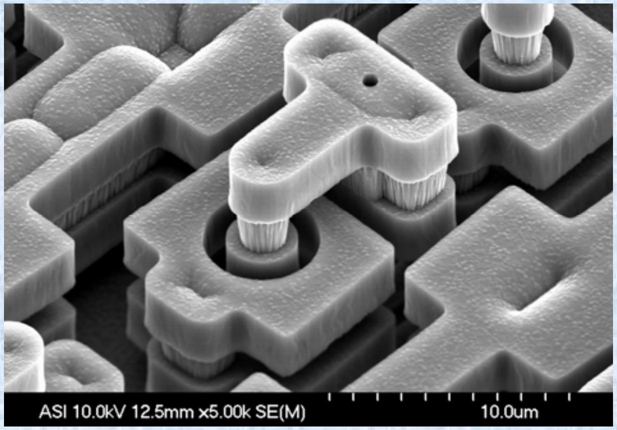

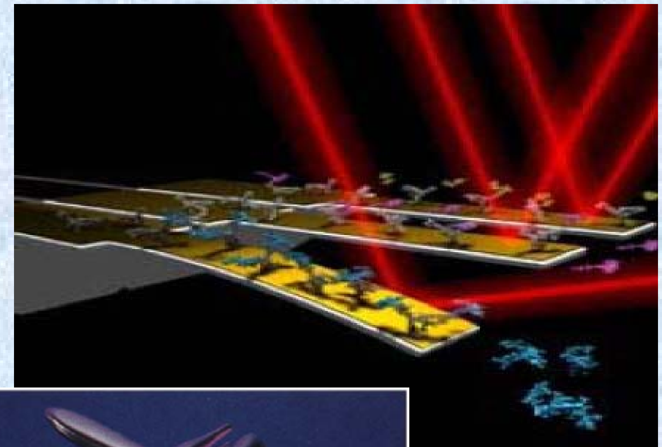

Thin Film Growth Technique - Sputtering

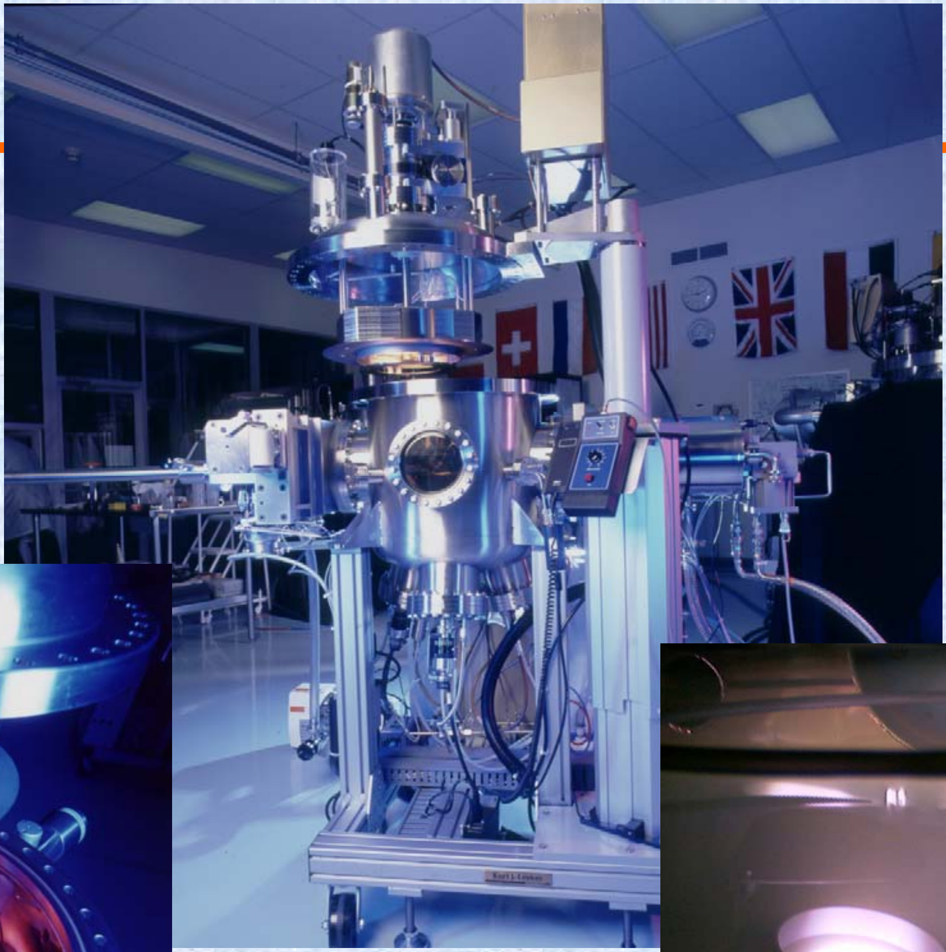

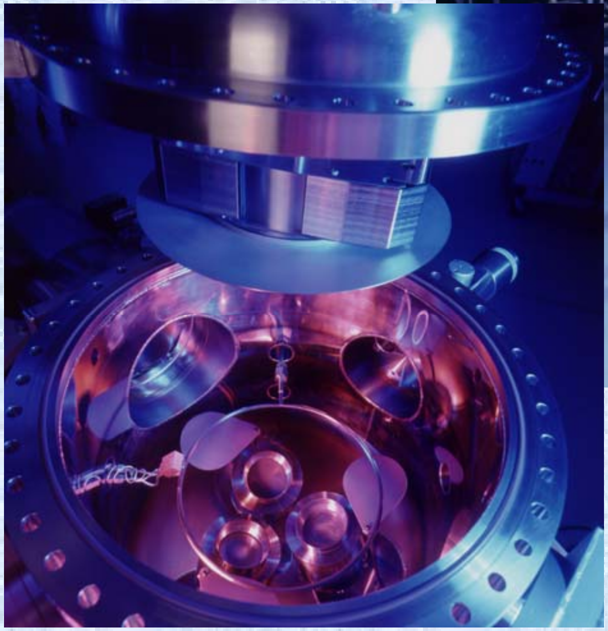

How to test film mechanical properties

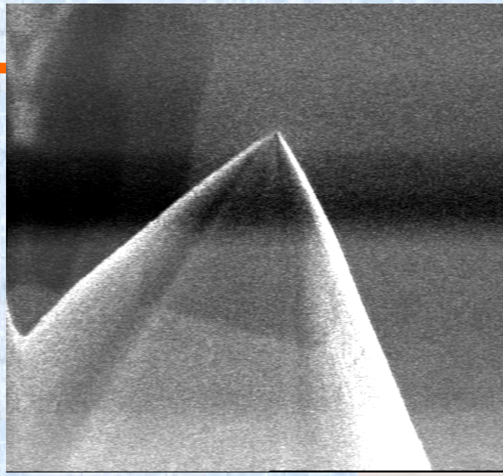

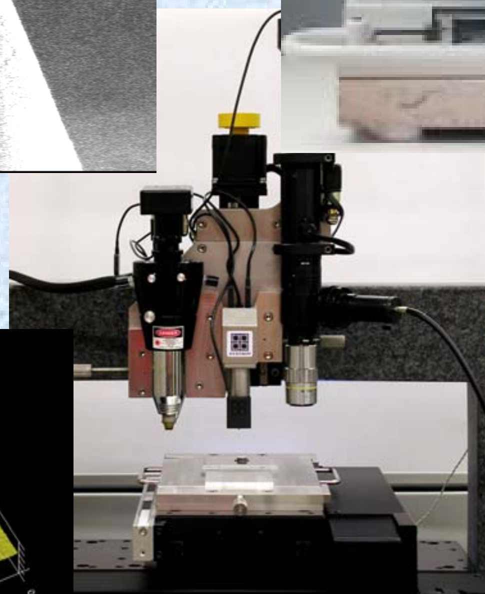

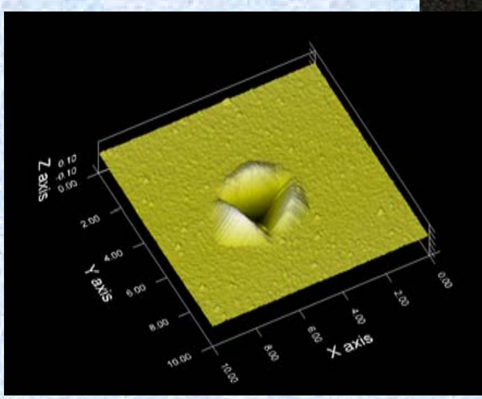

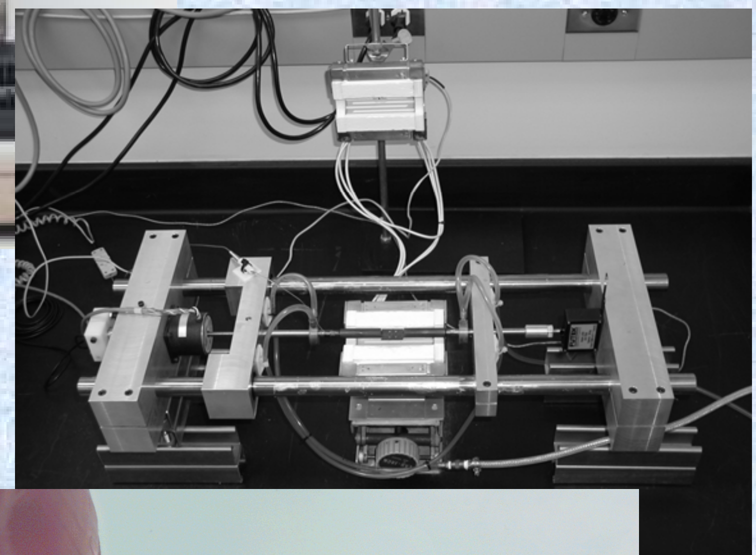

Nanoscale growth twins in sputtered 330SS films

Cross-sectional TEM

Growth

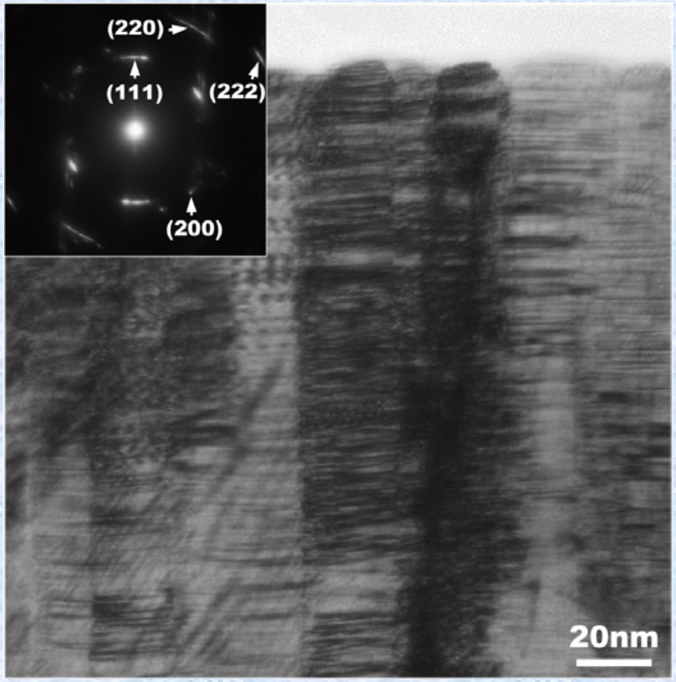

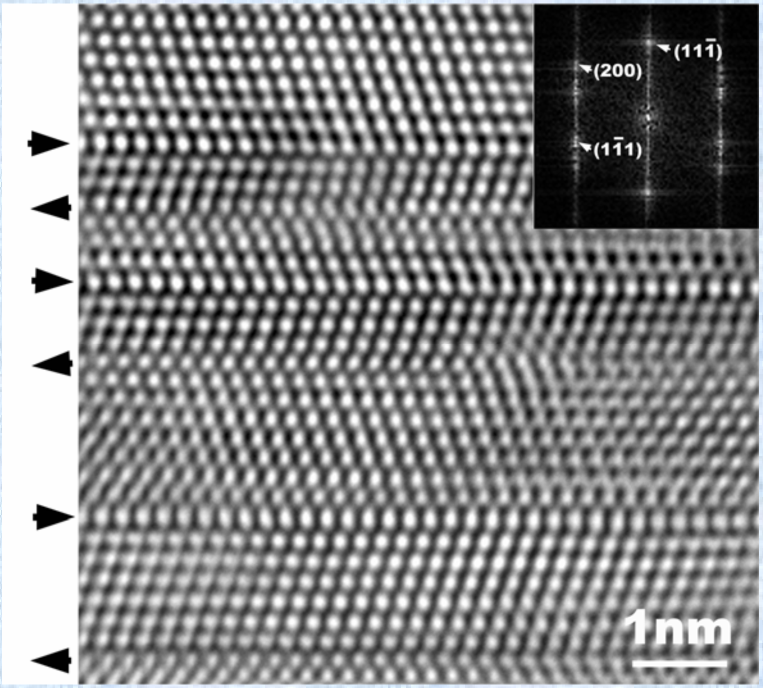

- fcc structure with {111} texture
- average columnar grain size ~ 30 nm
- {111} twin interface // substrate surface
- average twin spacing ~ 4 nm

Zhang et al, APL (2004).

Hardness of sputtered 330SS films is about an order of magnitude higher than that of bulk 330 SS

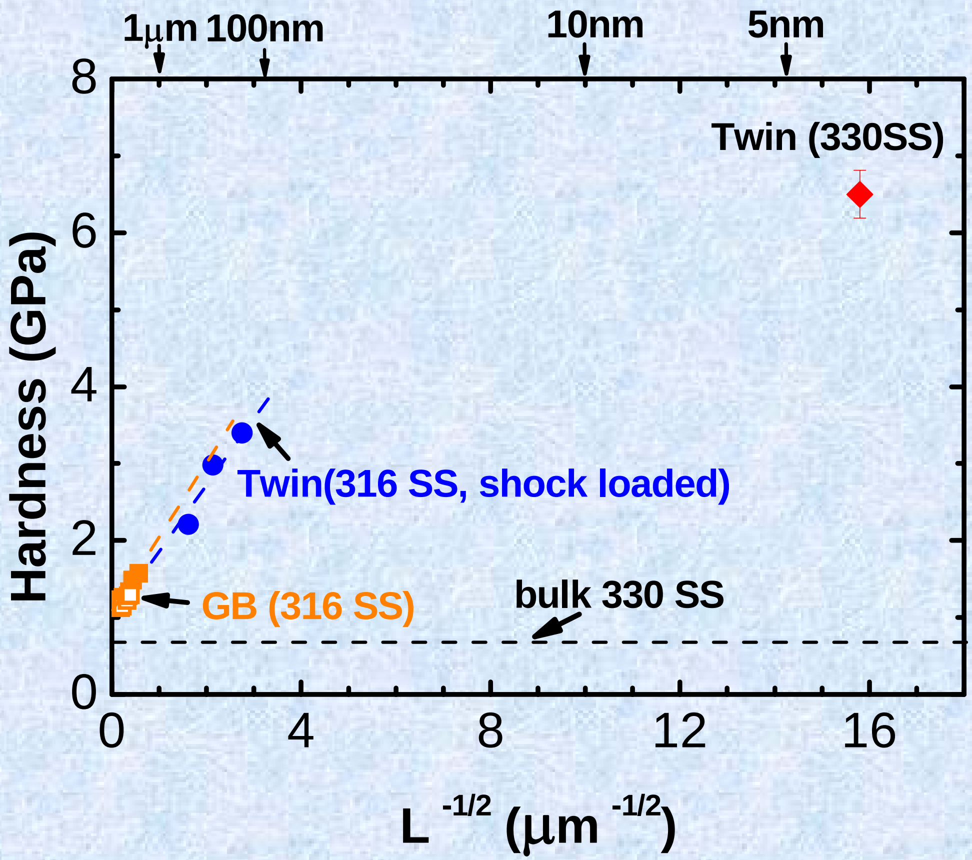

L - the smaller one of grain size or twin spacing

1. L. E. Murr et al, Scripta Metall., **12** (1978) 1031. (shock loaded SL)
2. Kashyap & Tangri, Acta Metall. Mater., **43** (1995) 3971. (GB strength)
3. K. J. Kurzydlowski, et al, Mater. Sci. Eng. **A205** (1996) 127. (GB strength)

Fundamental questions

- What is the role of twin interface in strengthening metallic thin films?
- How to tailor the formation of growth twins?

MD simulation of the resistance to shear in Ni (111) twin interface – pure shear stress

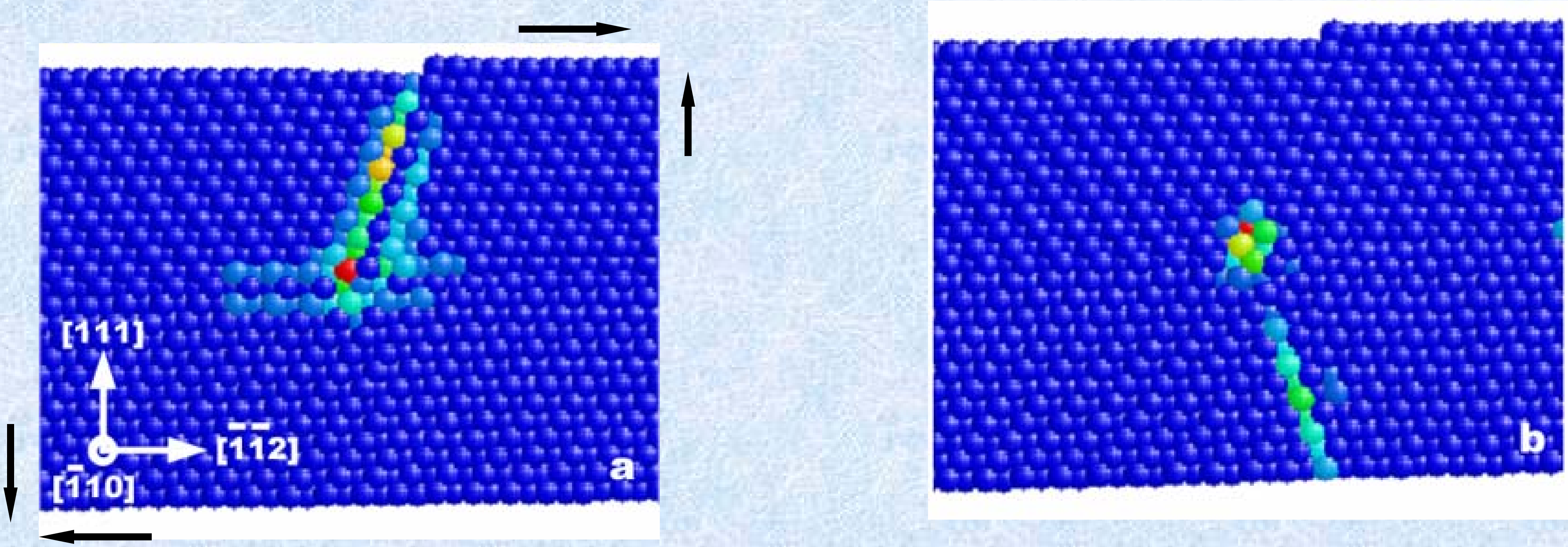

- **A resolved shear stress of 1.77 GPa is needed to move single dislocation (b = 1/2 [101]) across the twin interface to the lower {111} glide plane.**

Zhang et al, APL (2004).

Critical radius of twinned nuclei

No twin case

$$\Delta G_1 = 2\pi r h \gamma - \pi r^2 h \Delta G_V \Rightarrow r^*_{perfect} = \frac{\gamma}{\Delta G_v}$$

Twin case

$$\Delta G_2 = 2\pi r h \gamma - \pi r^2 h \Delta G_V + \pi r^2 \gamma_t \Rightarrow r^*_{twin} = \frac{\gamma}{\Delta G_v - \frac{\gamma_t}{h}}$$

$$\Delta G_v = \frac{kT}{\Omega} \ln\left(\frac{P_v}{P_s}\right) \qquad J = \frac{P_v}{\sqrt{2\pi m k T}}$$

(J - deposition rate)

Lower γ_t
or Higher J

$$\Rightarrow r^*_{perfect} \approx r^*_{twin}$$

Zhang, et al., Acta Mater. (2004)

At a deposition rate of a few Å/s, Δr/r < 10%

$$\Delta r / r = (r^*_{twin} - r^*_{perfect}) / r^*_{twin}$$

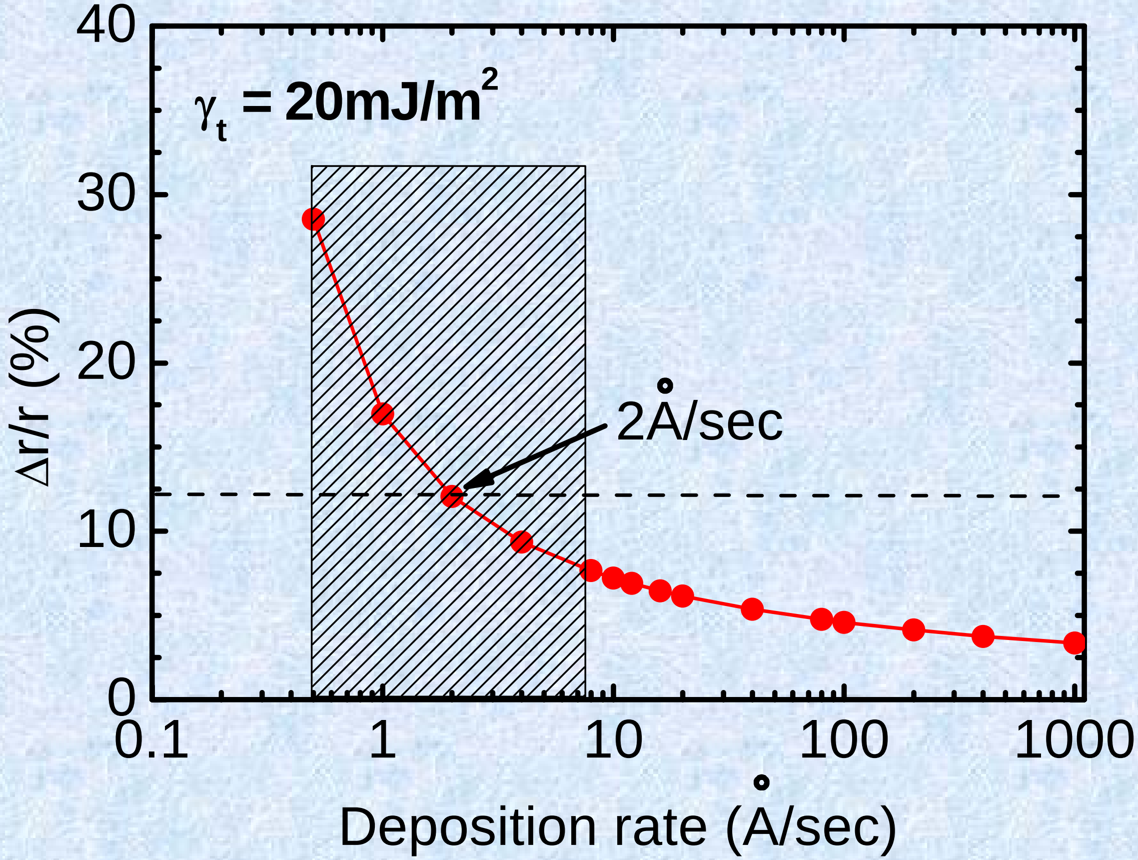

Hypothesis

Growth twins will have a higher probability to form if the deposition rate is higher ?

Experimental

- Magnetron sputtering (varying deposition rate)
- Hardness – nanoindentation
- Residual stress - curvature measurement with laser
- Microstructure - TEM

Deposition rate increases with deposition power

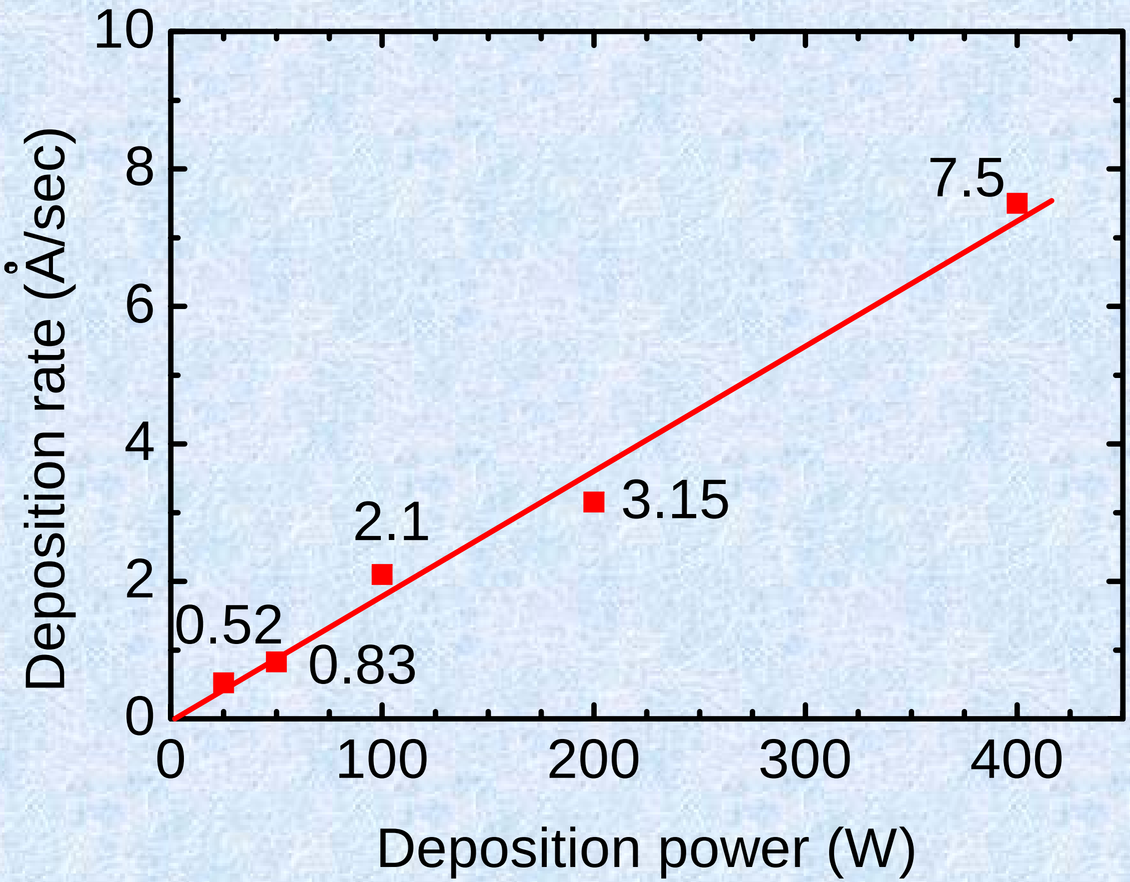

Microstructure of 330 SS films

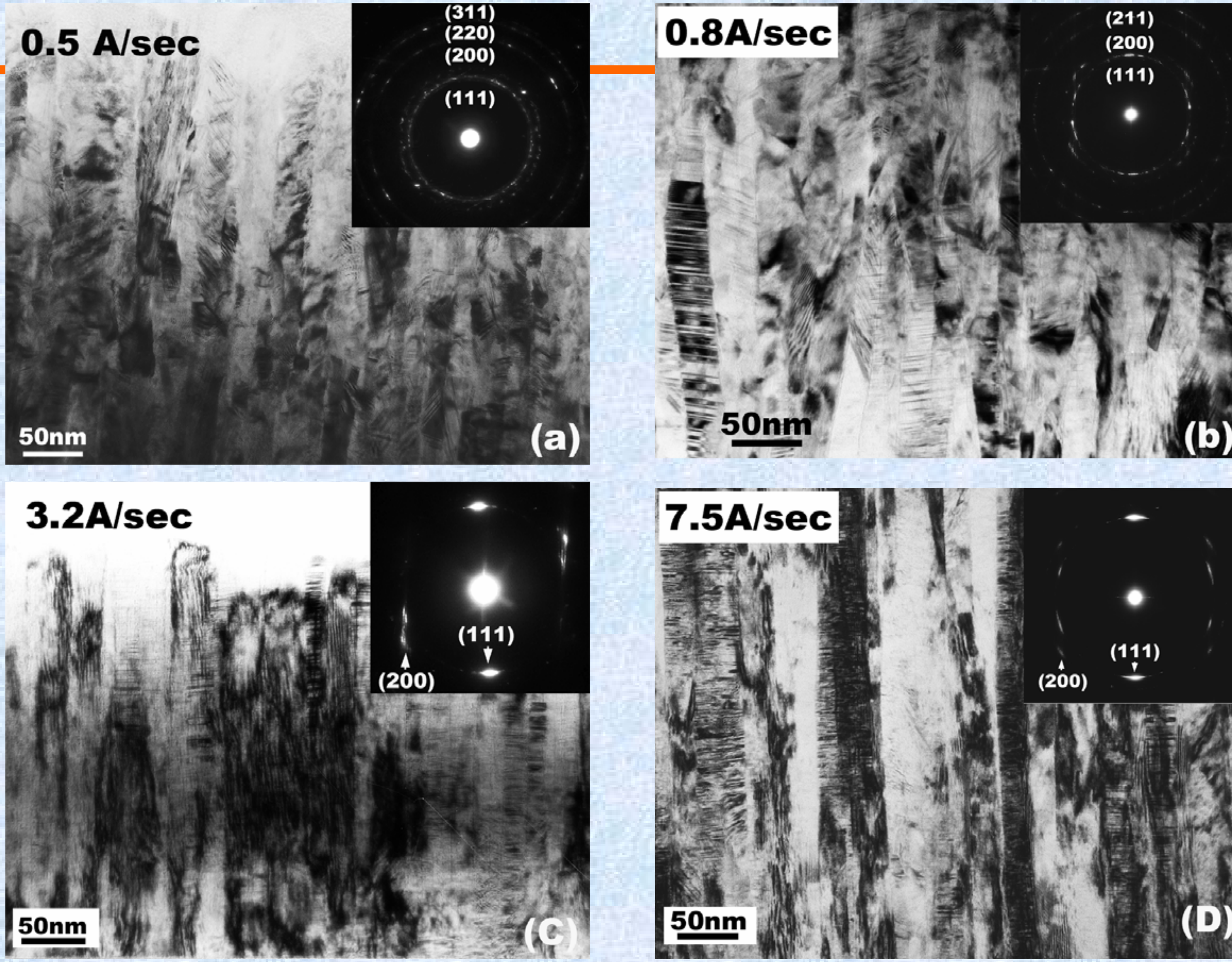

Microstructure evolutions

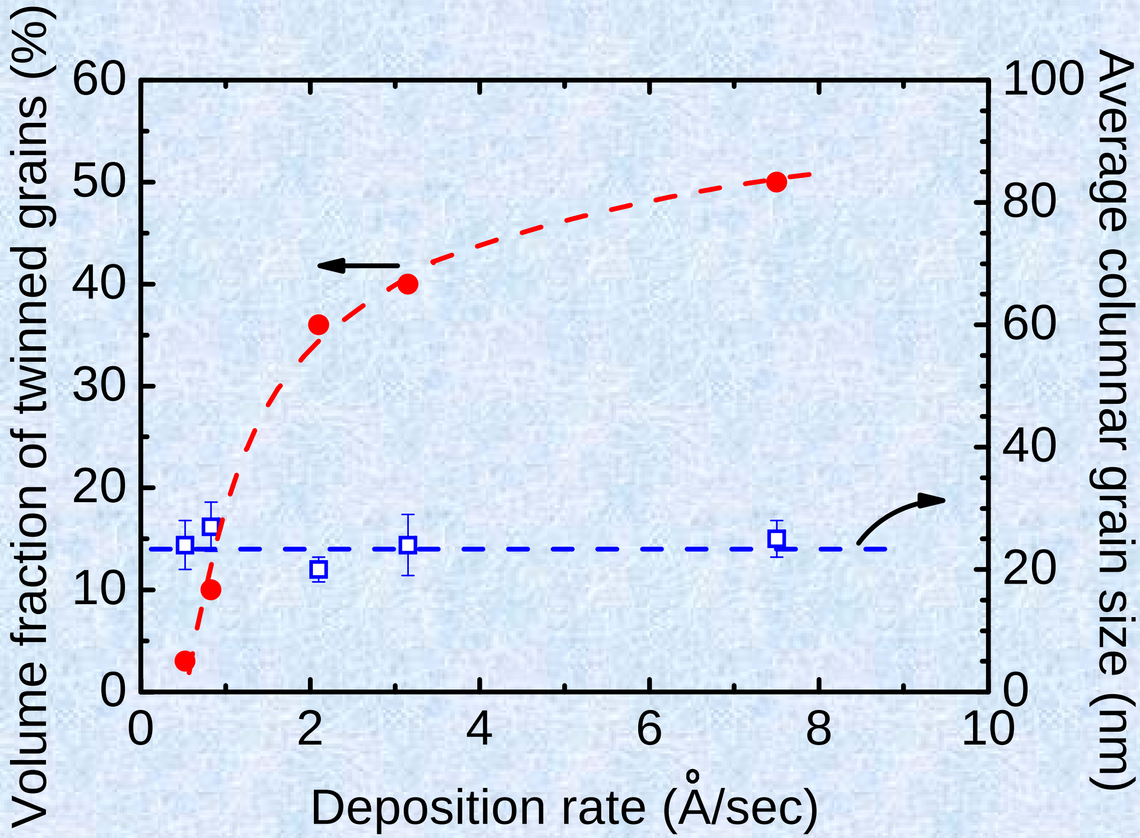

- The average twin spacing stays constant

Evolution of film hardness with the volume fraction of twinned materials

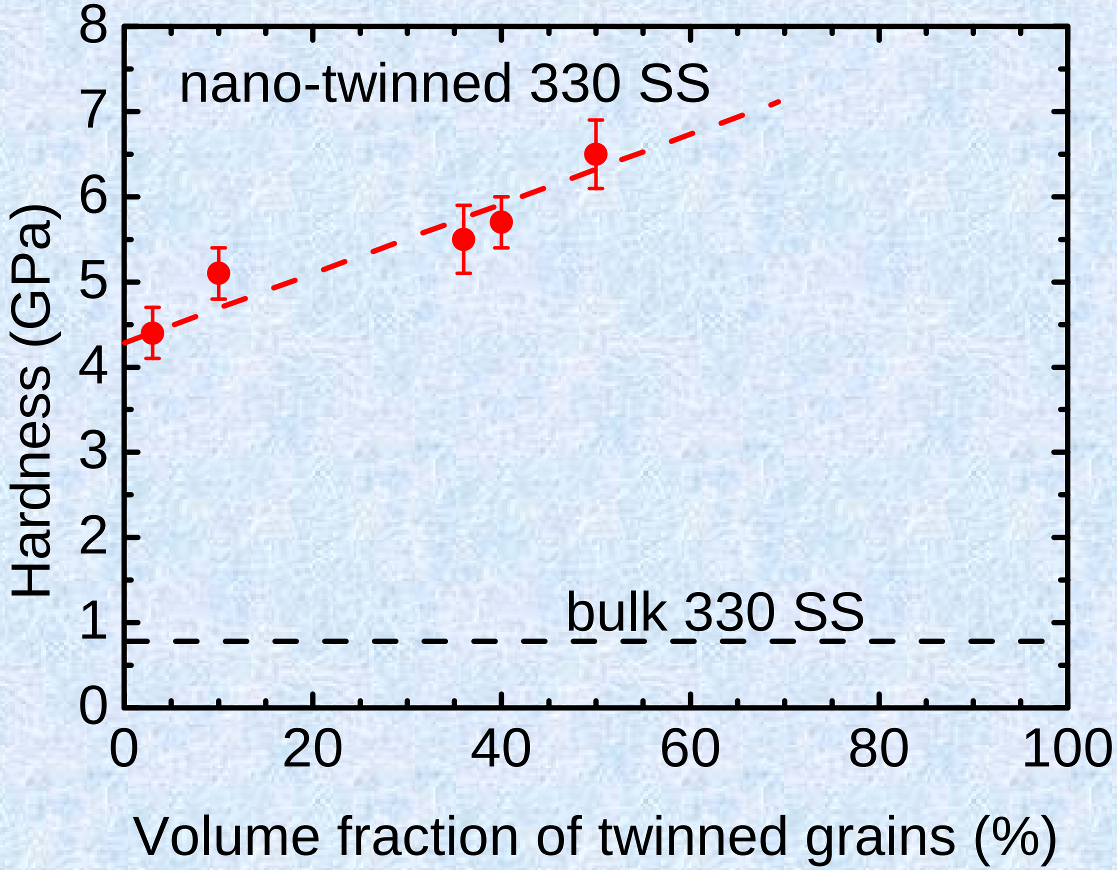

Outline

- Background
- Influence of sputtering deposition rate on twin formation in 330 stainless steel thin films
- Nanoscale growth twins in sputter-deposited Cu films

Nanoscale growth twins in electrodeposited Cu

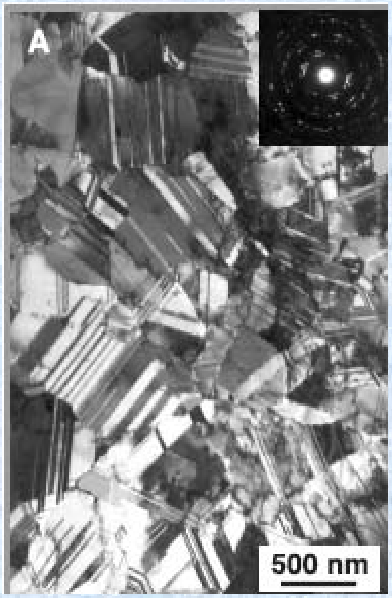

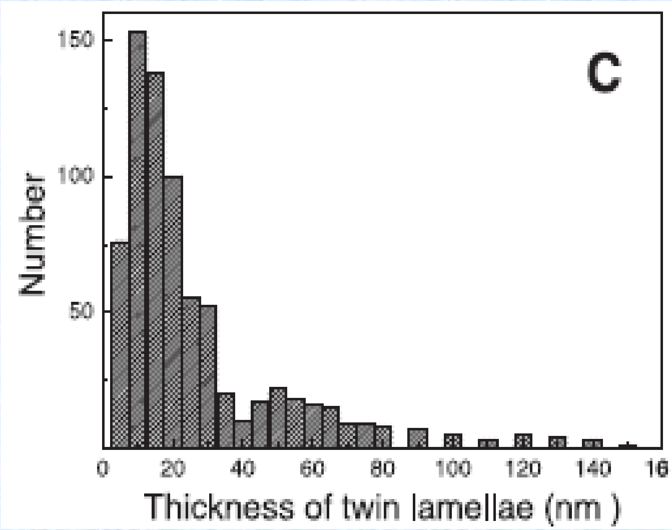

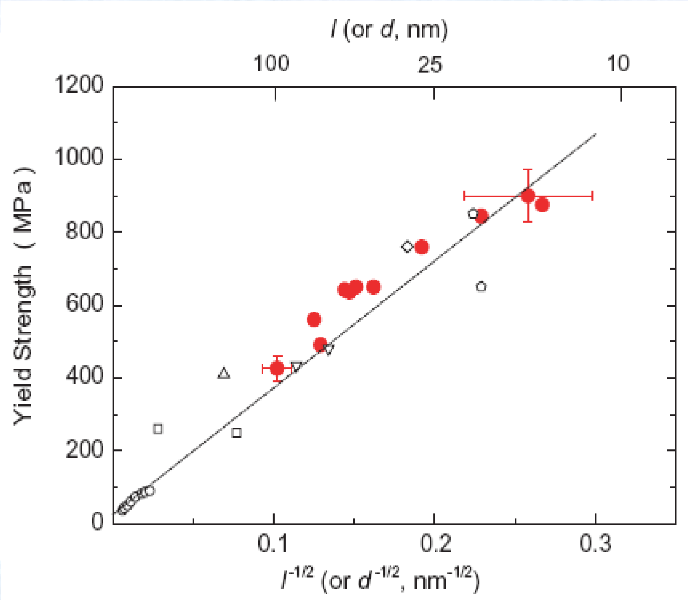

- **Minimum average twin spacing ~ 15 nm.**
- **Can we produce Cu with even smaller twin spacing using magnetron sputtering?**

L. Lu, Y. Shen, X. Chen, L. Qian, K. Lu, Science, **304**, 422 (2004).
Y.F. Shen, L. Lu, Q.H. Lu, Z.H. Jin, K. Lu, Scripta Mater. **52,** 989 (2005).

Plan view TEM micrograph of sputter-deposited Cu films

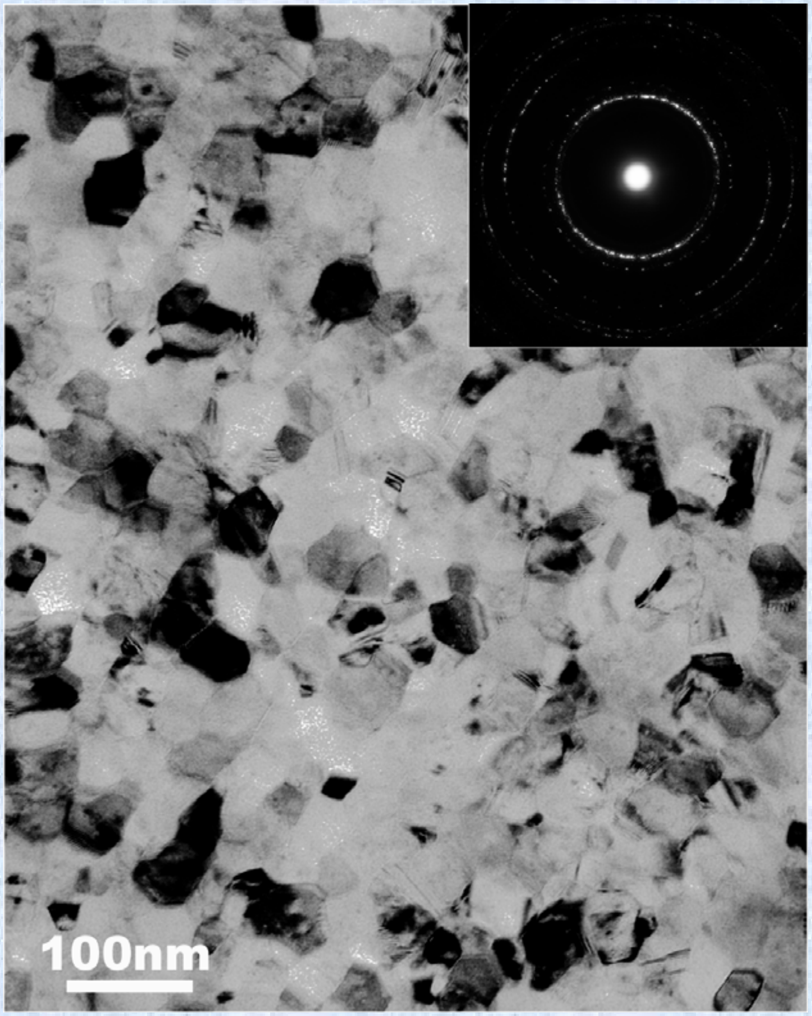

Cross-sectional TEM micrograph of sputtered Cu films

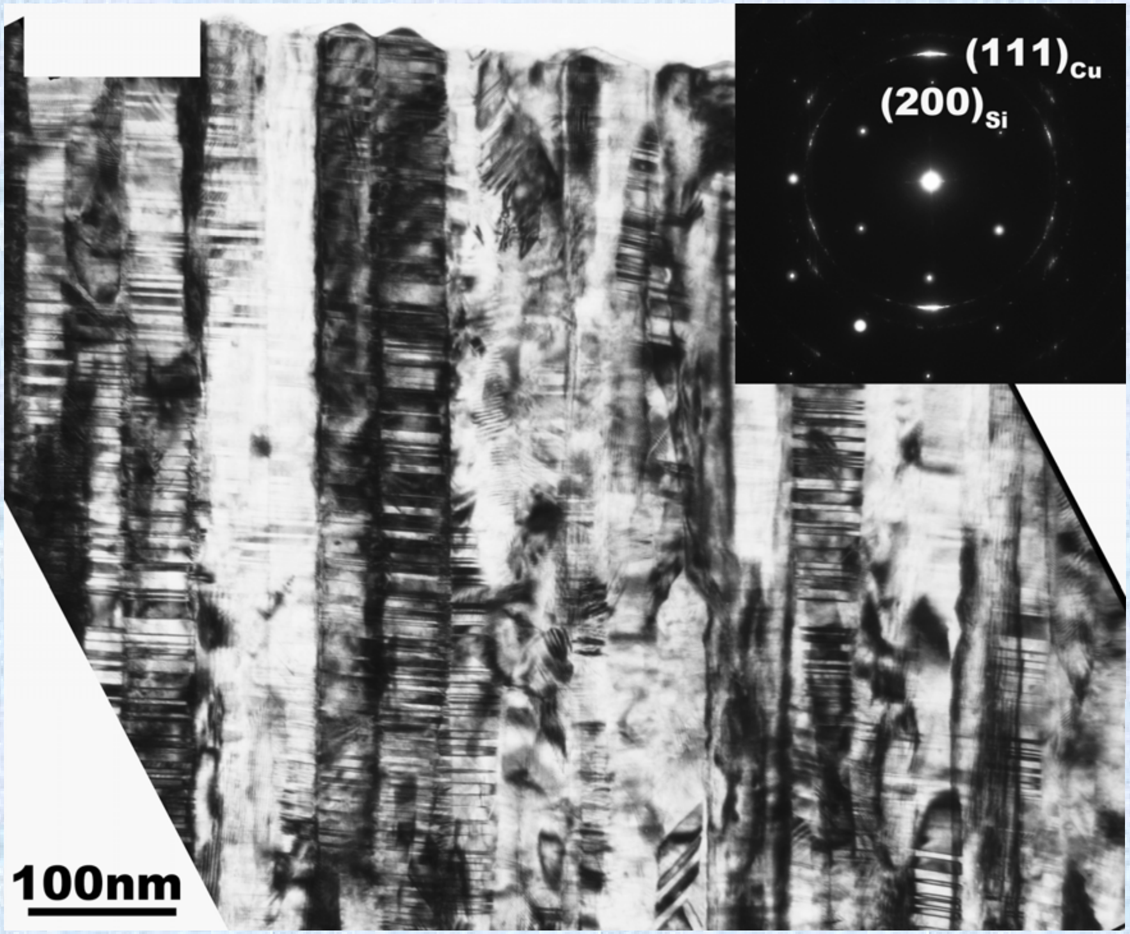

- High density planar defects
- {111} texture
- Average columnar grain size ~ 50 nm

Twin interface has preferred orientation (// film surface)

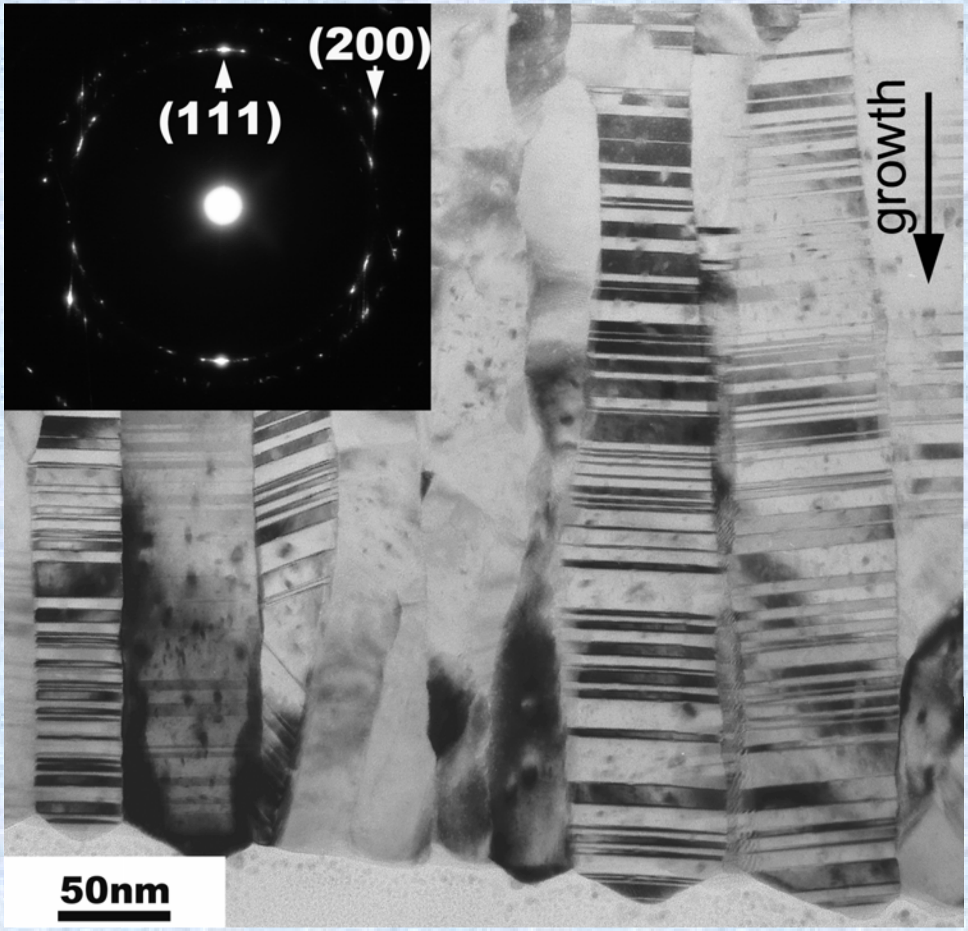

X. Zhang et al, APL, 2006

Coherent {111} twin interface with small twin spacing

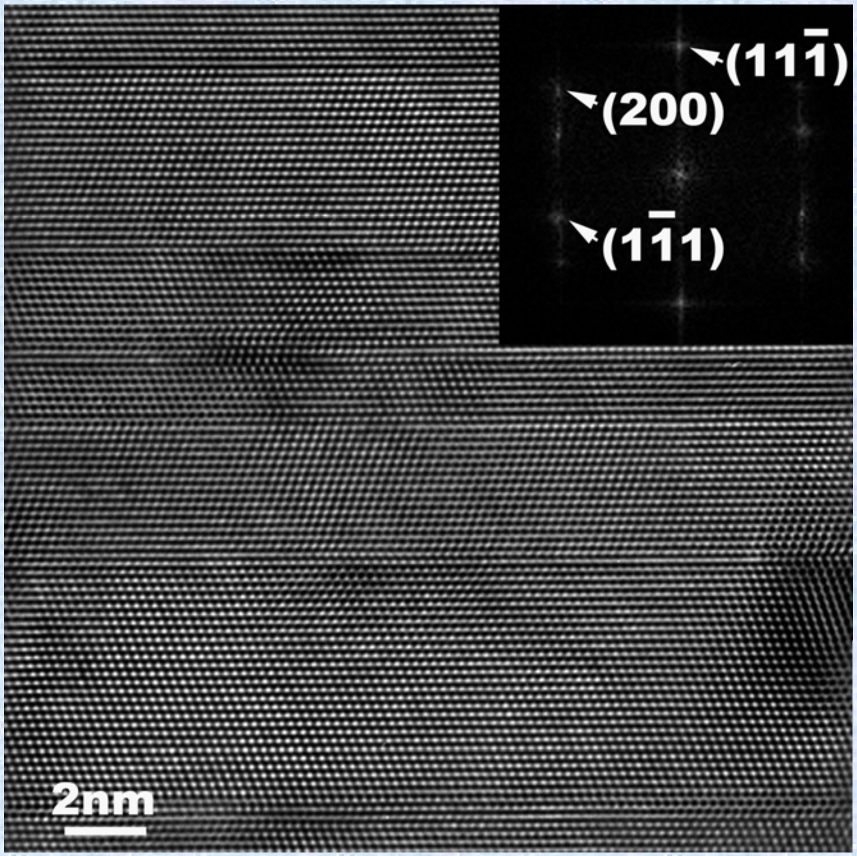

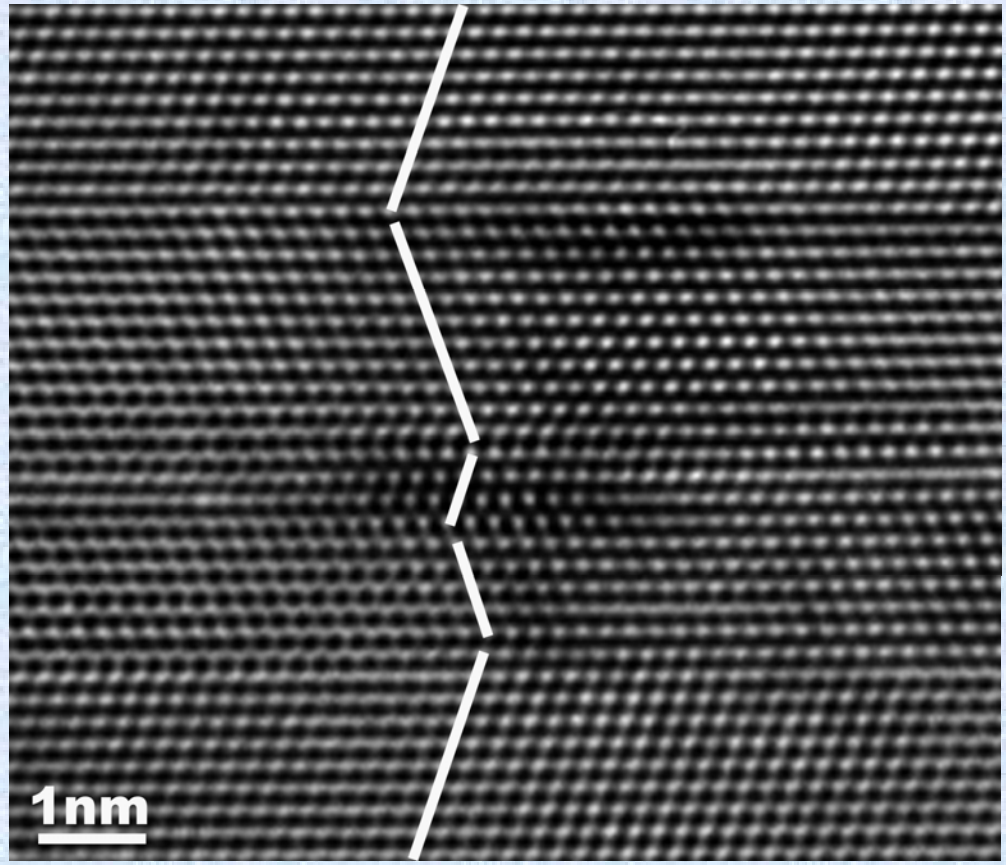

Average twin spacing and thickness are less than 10 nm (sputtered Cu films)

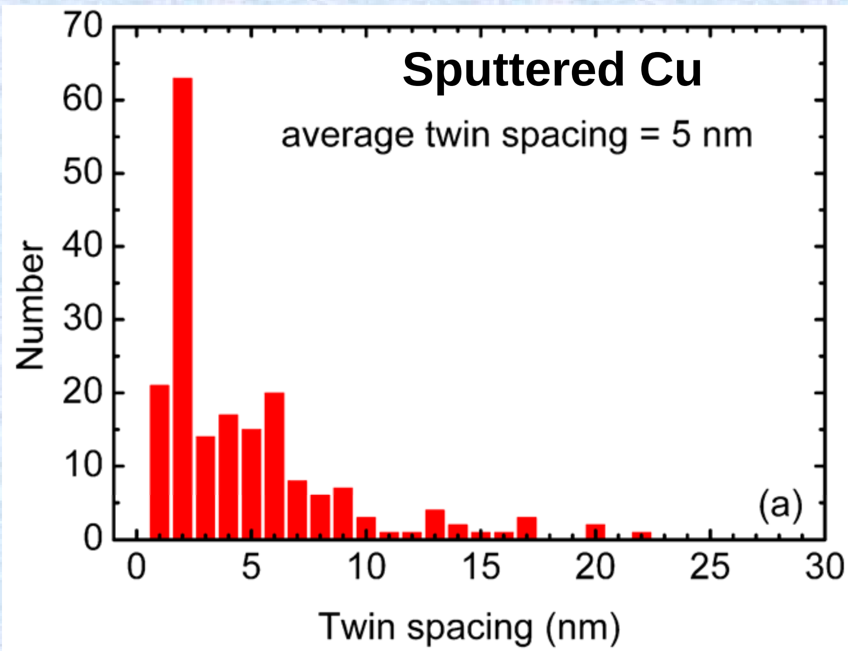

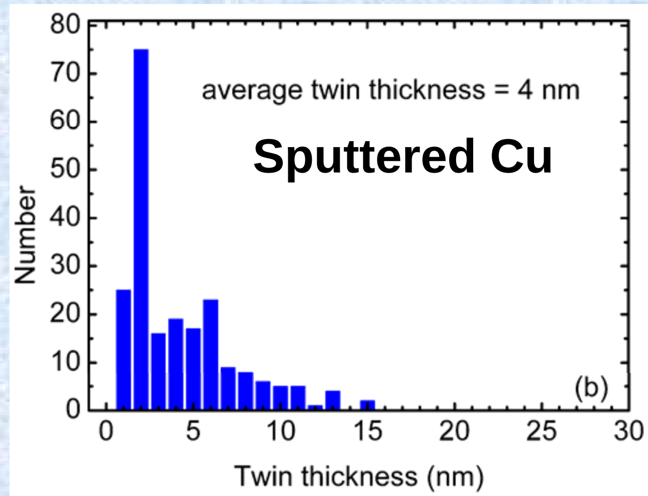

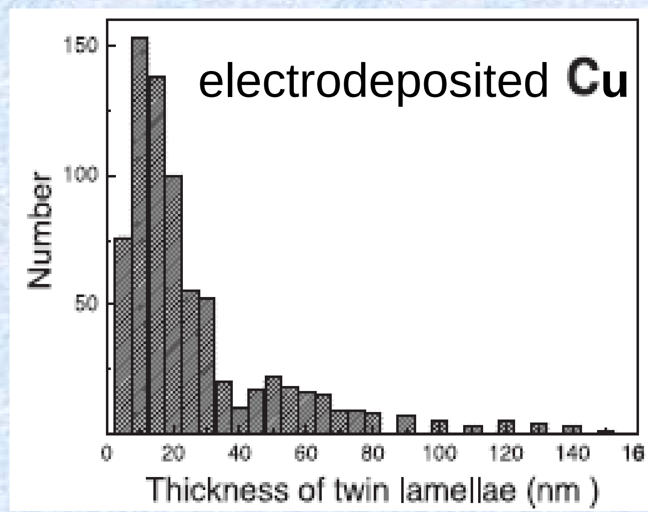

Film hardness = 3.5 GPa

Uniaxial tensile test of sputtered Cu foils (σ_y = 1.1 GPa, 1-2% uniform elongation)

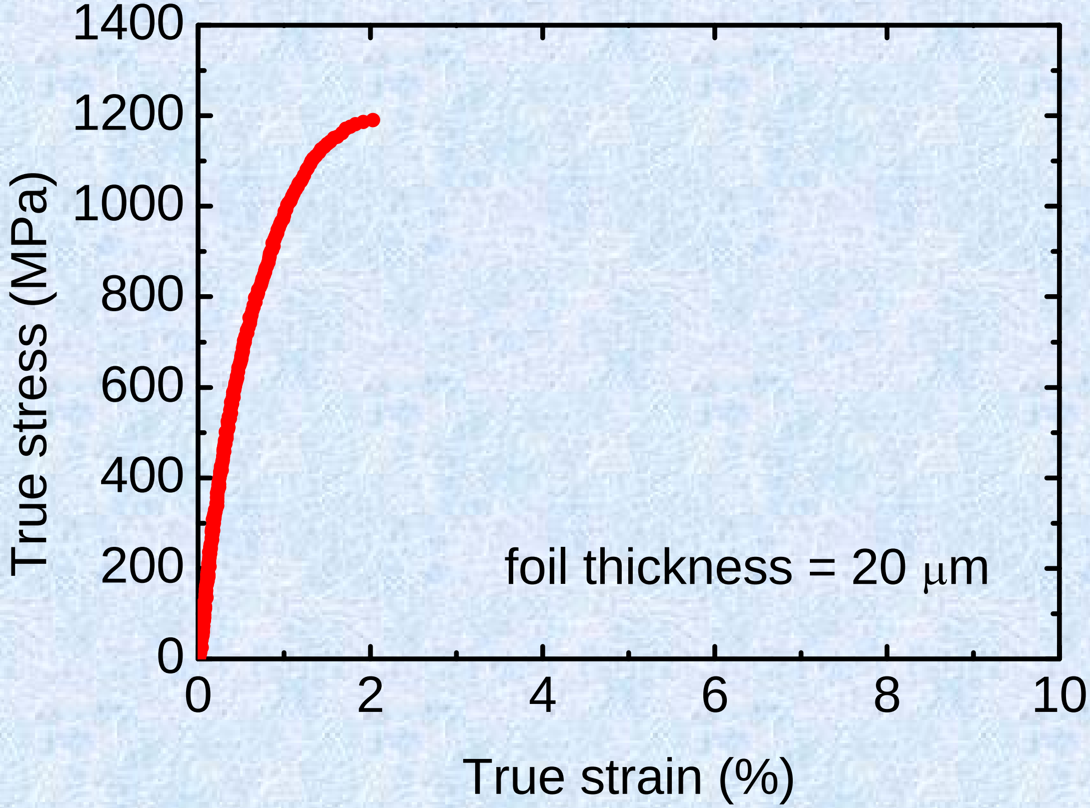

Fracture surface of Cu specimen

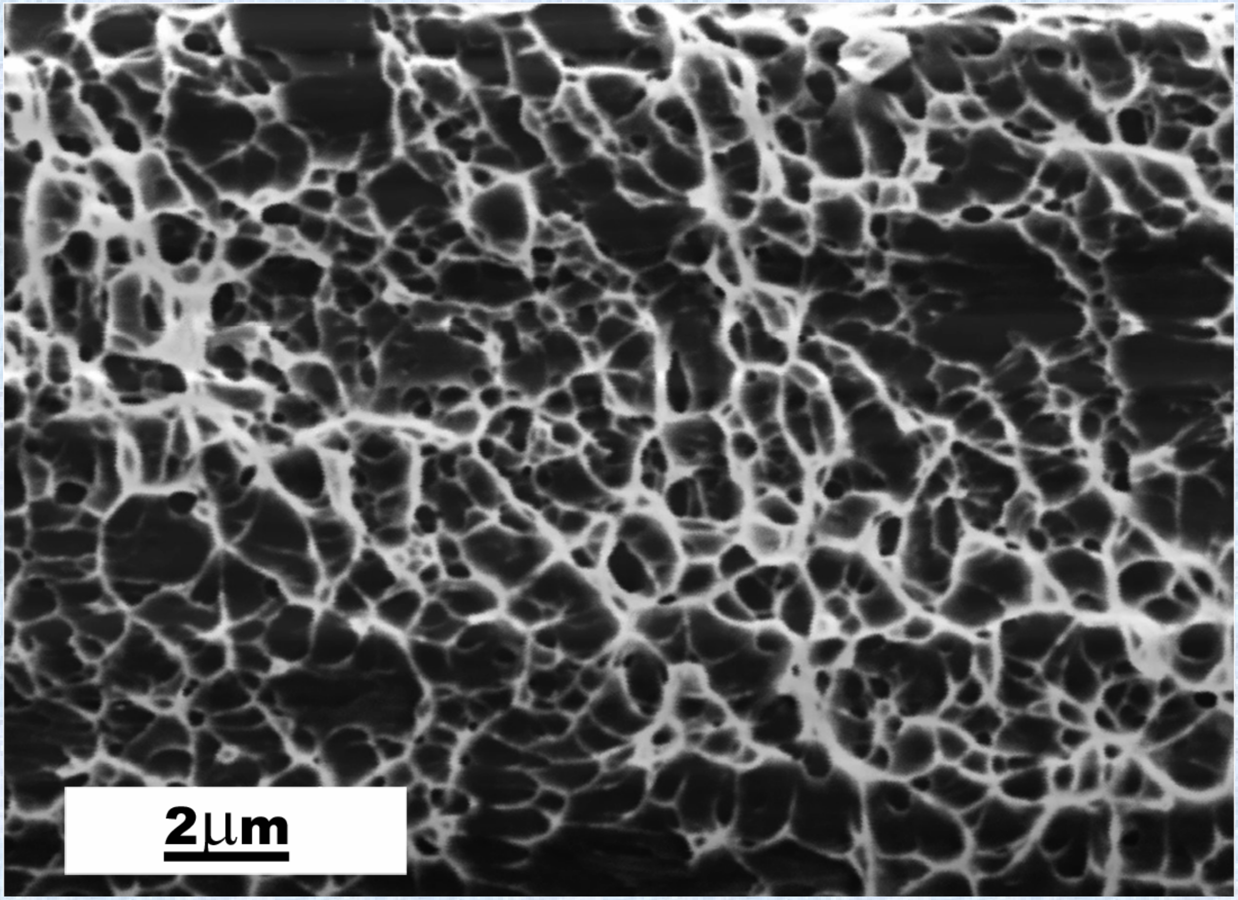

Influence of twin spacing on yield strength of twinned Cu

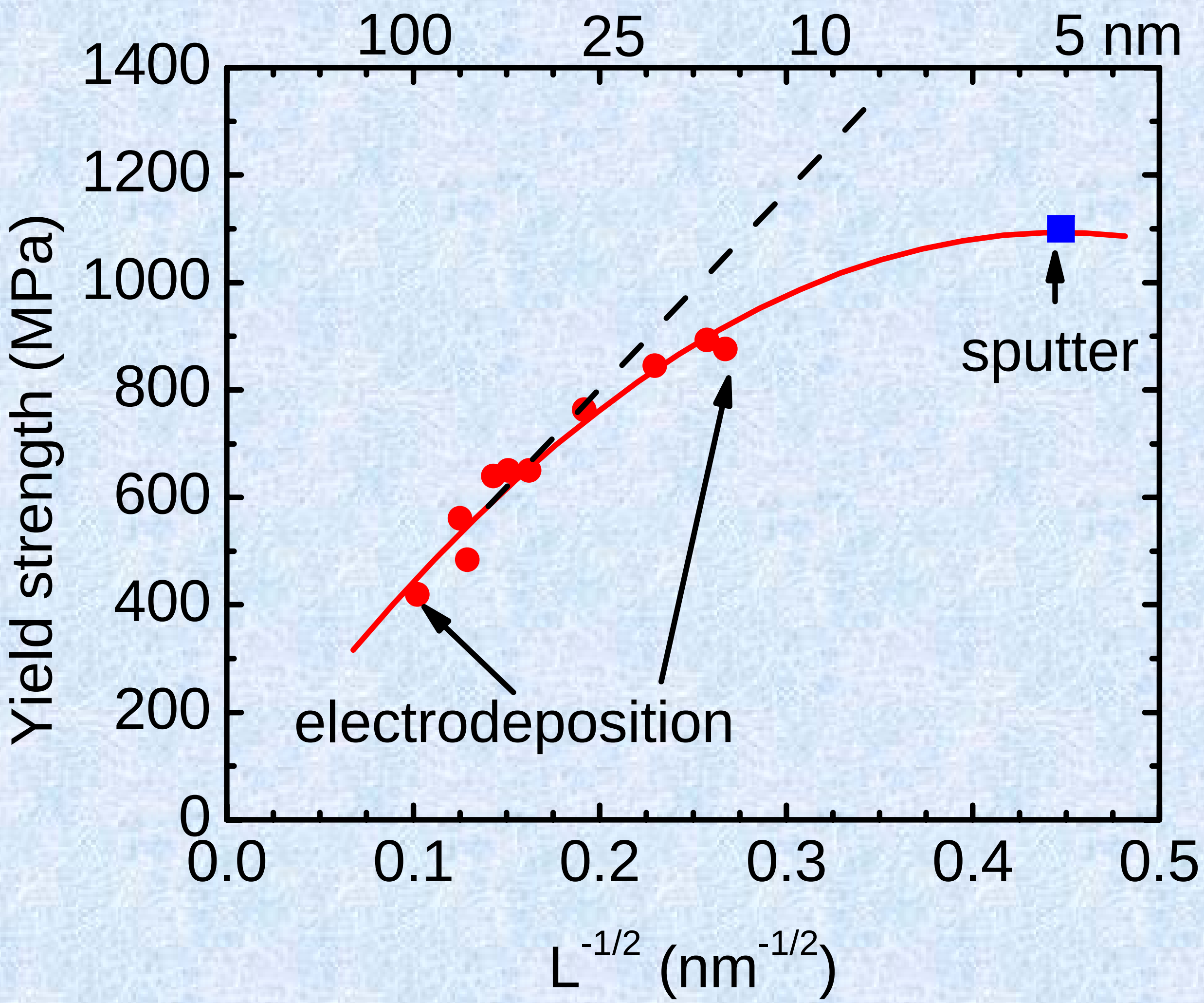

Summary - sputtered 330 SS films

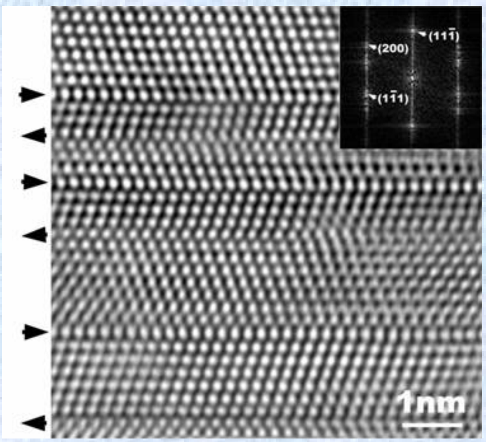

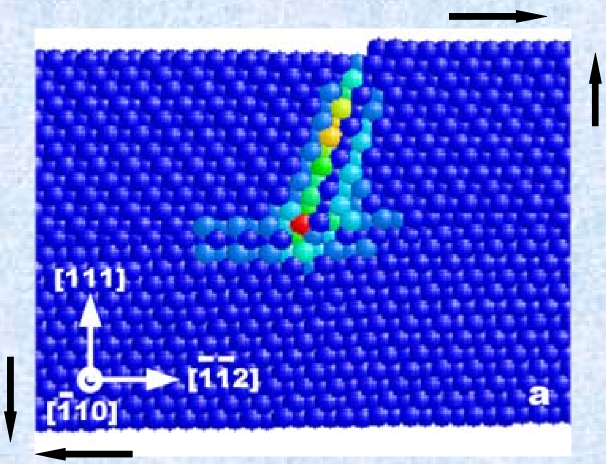

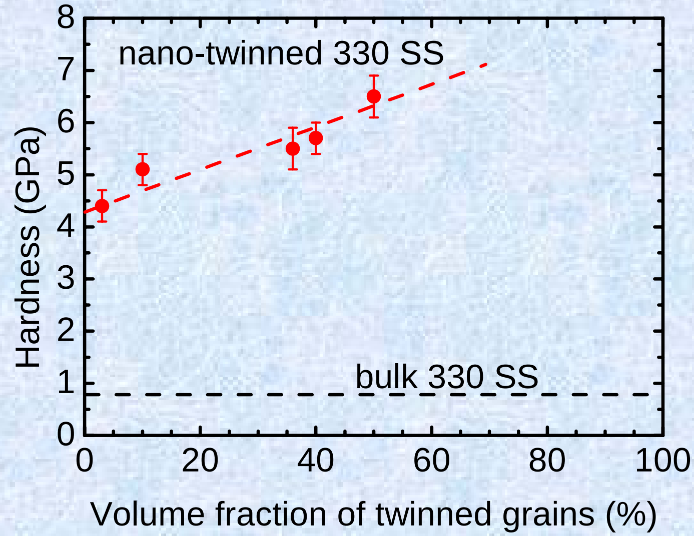

- Nanoscale growth twins strengthen 330 SS by an order of magnitude.
- Higher deposition rate leads to greater volume fraction of growth twins, and higher mechanical strength.

Summary- sputtered Cu films

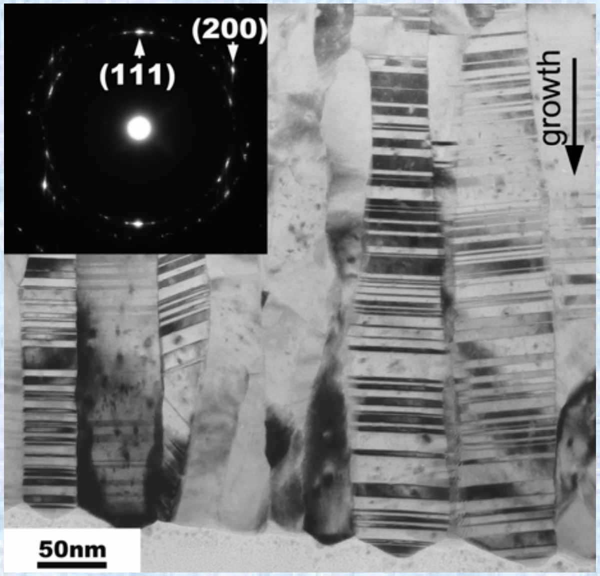

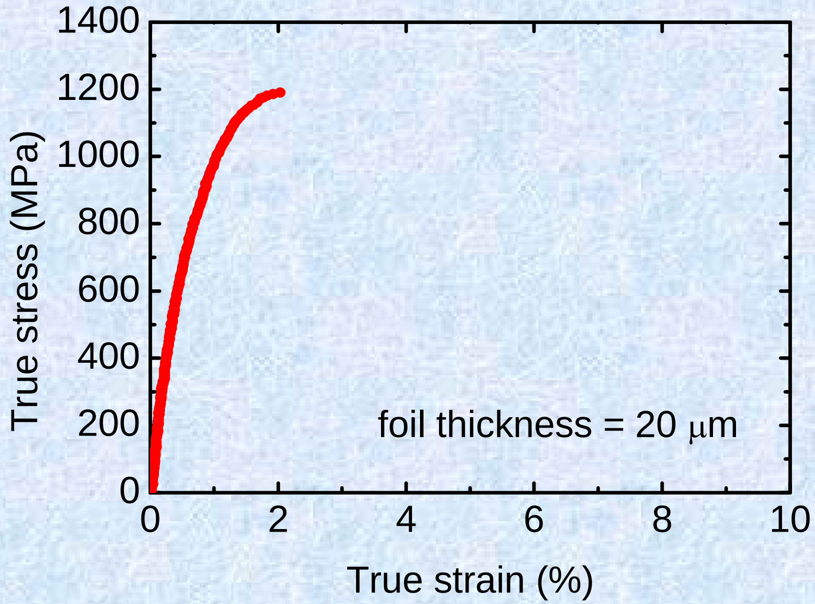

- {111} twins with an average twin spacing of a few nm
- Yield strength exceeding 1 GPa
- 1-2% uniform tensile elongation

Future plans

- Thermal stability of nanotwinned materials
- Deformability of nanotwinned Cu
- Crack propagation, wear and fatigue properties
- Electrical properties
- Synthesizing growth twins in high stacking-fault-energy metals (Ni, Al etc.)